Journal of Controlled Release 381 (2025) 113626

Contents lists available at ScienceDirect

Journal of Controlled Release

journal homepage: www.elsevier.com/locate/jconrel

Photopharmacological activation of adenosine A_1 receptor signaling suppresses seizures in a mouse model for temporal lobe epilepsy

Jeroen Spanoghe [a], Evelien Wynendaele [d], Marijke Vergaelen [a], Maren De Colvenaer [a], Tina Mariman [a], Kristl Vonck [a], Evelien Carrette [a], Wytse Wadman [a], Erine Craey [a], Lars E. Larsen [a], Mathieu Sprengers [a], Jeroen Missinne [b], Serge Van Calenbergh [c], Bart De Spiegeleer [d], Dimitri De Bundel [e], Ilse Smolders [e], Paul Boon [a], Robrecht Raedt [a,*]

[a] 4Brain, Department of head and Skin, Ghent University, Corneel Heymanslaan 10, 9000 Ghent, Belgium
[b] Centre for Microsystems Technology (CMST), Department of Electronics and Information systems, imec and Ghent University, Technologiepark 126, 9052 Ghent, Belgium
[c] Laboratory for Medicinal Chemistry, Department of Pharmaceutics, Ghent University, Ottergemsesteenweg 460, 9000 Ghent, Belgium
[d] Drug Quality and Registration (DruQuaR) group, Department of Pharmaceutical Analysis, Ghent University, Ottergemsesteenweg 460, 9000 Ghent, Belgium
[e] Center for Neurosciences, Research Group Experimental Pharmacology, Department of Pharmaceutical and Pharmacological Sciences, Vrije Universiteit Brussel, Laarbeeklaan 103, 1090 Jette, Belgium

ARTICLE INFO

Keywords:
Photopharmacology
Photo-uncaging
Adenosine
Adenosine A_1 receptor
Epilepsy
Drug-resistant epilepsy
Temporal lobe epilepsy

ABSTRACT

Up to 30 % of epilepsy patients suffer from drug-resistant epilepsy (DRE). The search for innovative therapies is therefore important to close the existing treatment gap in these patients. The adenosinergic system possesses potent anticonvulsive effects, mainly through the adenosine A_1 receptor (A_1R). However, clinical application of A_1R agonists is hindered by severe systemic side effects. To achieve local modulation of A_1Rs, we employed a photopharmacological approach using a caged version of the A_1R agonist N^6-cyclopentyladenosine, termed cCPA. We performed the first *in vivo* study with intracerebroventricularly (ICV) administered cCPA to investigate the potential to photo-uncage and release sufficient amounts of cCPA in the hippocampus by local illumination in order to suppress hippocampal excitability and seizures in mice. We validated the presence of cCPA in the hippocampus after ICV injection and explored its pharmacokinetic profile and *in vivo* stability. Using hippocampal evoked potential recordings, we showed a reduction in hippocampal neurotransmission after photo-releasing CPA, similar to that obtained with ICV injection of CPA. Furthermore, in the intrahippocampal kainic acid mouse model for DRE, photo-release of CPA in the epileptic hippocampus resulted in a strong suppression of seizures. Finally, we demonstrated that intrahippocampal photo-release of CPA resulted in less impairment of motor performance in the rotarod test compared to ICV administration of CPA. These results provide a proof of concept for photopharmacological A_1R modulation as an effective precision treatment for DRE.

1. Introduction

Of the estimated 50 million epilepsy patients worldwide, more than one third suffers from drug-resistant epilepsy (DRE) [1–3]. In these patients, currently available antiseizure medication (ASM) fails to achieve seizure freedom or causes unacceptable side effects. In the search for innovative therapies to close the existing treatment gap in epilepsy patients, adenosine receptor agonists have been the subject of many preclinical studies [4–11]. The adenosinergic system plays an important endogenous anticonvulsive role in the central nervous system (CNS). Extracellular adenosine concentrations have been shown to rise during seizures [12–14], which is hypothesized to be an important factor for the spontaneous termination of seizures. These seizure-suppressive effects of adenosine can mainly be attributed to binding of adenosine to the adenosine A_1 receptor (A_1R) subtype. Activation of this G_i-coupled receptor leads to a suppression of neurotransmitter release through inhibition of voltage-gated Ca^{2+} channels and a decrease in neuronal excitability by opening of K^+ channels, causing membrane

* Corresponding author.
E-mail address: Robrecht.Raedt@UGent.be (R. Raedt).

https://doi.org/10.1016/j.jconrel.2025.113626
Received 2 July 2024; Received in revised form 15 February 2025; Accepted 10 March 2025
Available online 12 March 2025

hyperpolarization [15]. Some of the highest expression levels of A_1Rs are found in the hippocampus [16], from which seizures often originate in case of temporal lobe epilepsy (TLE). As one of the most common forms of DRE [17], TLE therefore marks itself as an ideal target for adenosine-based interventions.

Administration of adenosine or A_1R agonists has been demonstrated to be effective in models for DRE [18,19]. However, clinical translation of such therapies is hindered by severe side effects of systemic administration, such as bradycardia and hypothermia, due to the ubiquitous expression of A_1Rs throughout the body. To take advantage of the strong seizure-suppressive effects of the A_1R, strategies are required that allow for local activation of these receptors at the site of the seizure focus. In the past, antiseizure effects have been achieved with chronic local delivery of adenosine *via* infusion with osmotic minipumps, implantation of adenosine-releasing polymers and genetically-engineered adenosine-releasing cells [8,20–24]. These strategies all involve a local but invariable, continuous increase of adenosine concentrations. We are now investigating a novel approach that has the potential to deliver a more controlled modulation of A_1Rs, namely photopharmacology.

Through a combination of photochemistry and pharmacology, the field of photopharmacology involves the use of light to provide high spatiotemporal control over the activity of drugs [25–27]. With the technique of "photocaging", a photoremovable protective group (or "photocage") is covalently bonded to a bioactive ligand, thereby rendering it inactive. Activity can be restored by breaking the photosensitive bond using illumination of a specific wavelength, a process called "photo-uncaging". Photopharmacology has become an emerging field of research and in recent years its therapeutic potential is increasingly being explored *in vivo*. For instance, photocaged compounds have been tested for control over metabotropic glutamate type 5 and opioid receptors in analgesia studies [28–30], the adenosine A_{2A} receptor in Parkinson's disease [31] and the adenosine A_3 receptor in psoriasis [32]. Yet, so far this technique has only seen limited application in epilepsy research. A first proof of concept for its therapeutic potential was delivered by Yang et al., who used local photo-uncaging of caged γ-aminobutyric acid to terminate paroxysmal activity induced by 4-aminopyridine in the neocortex of rats *in vitro* and *in vivo* [33,34].

For photopharmacological modulation of A_1R activity, we recently caged the A_1R agonist N^6-cyclopentyladenosine (CPA) with the coumarin-derivative 7-(diethylamino)-4-(hydroxymethyl)-2H-chromen-2-one (DEACM), which is sensitive to light of 405 nm wavelength [35] (Fig. 1). This caged CPA (cCPA) has previously been validated *ex vivo* in our laboratory and displays a 1000-fold reduced affinity for the A_1R compared to CPA [36]. In acute hippocampal brain slices, positioned on a multielectrode array (MEA) and superfused with 3 μM cCPA, illumination with millisecond flashes of 405 nm light at an intensity of 4 mW released an estimated concentration of 30 nM CPA. This was sufficient to suppress stimulation evoked potentials (EPs), which reflects a reduction in neurotransmission and neuronal excitability and thus indicated successful A_1R activation with cCPA. Furthermore, this approach was also capable of suppressing epileptiform bursts in the high-potassium hippocampal slice model [37].

In the present study, we explored the use of cCPA for the first time *in vivo*. We examined the hippocampal concentrations of cCPA after intracerebroventricular (ICV) administration and explored its pharmacokinetics and stability in brain tissue and blood using ultra-high performance liquid chromatography-mass spectrometry (UHPLC-MS). The possibility to uncage cCPA *in vivo* was investigated using local illumination through an implanted optical fiber in the hippocampus of anesthetized mice. We studied effects on hippocampal EPs similar to our previous *ex vivo* study, where a reduction in EPs reflects A_1R activation. These hippocampal EPs were evoked by electrical stimulation of presynaptic axons of the perforant path (PP), which causes depolarization of postsynaptic granule cells in the dentate gyrus (DG) resulting in a field excitatory postsynaptic potential (fEPSP) [38]. Synchronous generation of action potentials in the granule cells induces a "population spike (PS)", which is represented as a negative deflection on the fEPSP (Fig. 2).

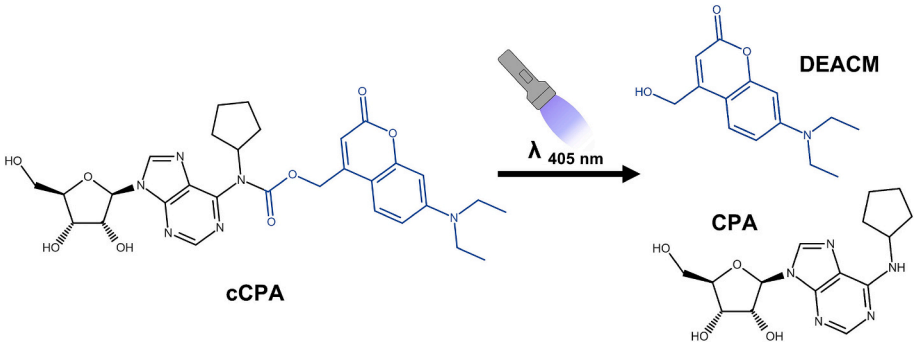

Fig. 1. Structure of caged CPA (cCPA) and schematic representation of its uncaging into CPA and DEACM after exposure to 405 nm illumination. CPA: N^6-cyclopentyladenosine; DEACM: 7-(diethylamino-4-(hydroxymethyl)-2H-chromen-2-one.

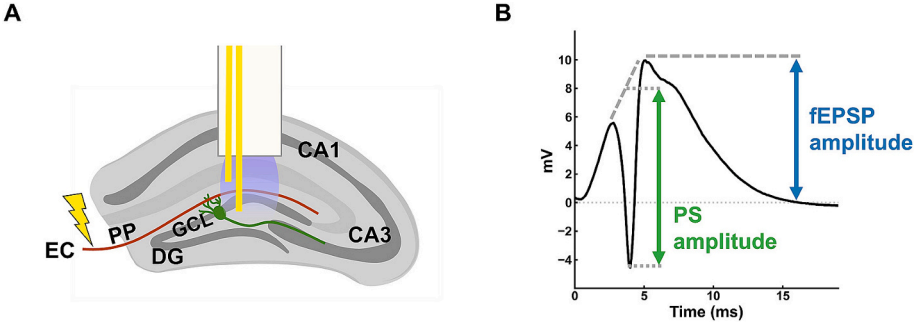

Fig. 2. (**A**) Illustration of the hippocampus with an optrode implanted for evoked potential (EP) recording. Electrical stimulation of the perforant path elicits EPs in the granule cell layer of the dentate gyrus. (**B**) Example of a hippocampal EP constituting of a positive field excitatory post-synaptic potential (fEPSP) and a negative population spike (PS). CA: cornu ammonis; DG: dentate gyrus; EC: entorhinal cortex; GCL: granule cell layer; PP: perforant path.

Next, we investigated whether local A_1R activation with this photopharmacological approach can be used to suppress seizures in the intrahippocampal kainic acid (IHKA) mouse model, which displays chronic recurrent hippocampal seizures that are resistant to several frequently used ASMs [39,40]. To this end, effects on seizure frequency were examined after ICV administration of cCPA combined with local hippocampal illumination. Additionally, we investigated possible effects of our photopharmacological treatment on locomotor activity, as administration of A_1R agonists is known to cause sedation [41,42]. Since we aim to achieve a more spatially controlled activation of A_1Rs with cCPA in order to avoid such side effects, we compared the effects between CPA administration and photo-release of CPA on the performance of mice on the accelerating rotarod test.

2. Material & methods

2.1. Chemicals

The A_1R agonist N^6-cyclopentyladenosine (CPA) was acquired from Tocris Bioscience (Bristol, UK). The DEACM used as photocage was acquired from Sigma-Aldrich (Saint Louis, USA). Photocaged CPA (cCPA) was synthesized as previously reported [36]. Dimethylsulfoxide (DMSO, Tocris Bioscience) was used as solvent for both CPA and cCPA. Solutions containing cCPA were prepared in the dark and shielded from ambient light during all experiments.

2.2. Animals

Experiments were performed in adult male C57Bl/6 J mice (8 weeks old at the start of experiments), obtained from Envigo (The Netherlands). Animals were housed under environmentally controlled conditions (temperature 21–22 °C, relative humidity 40–60 %) at a fixed 12-h light/dark cycle. Food and water were available *ad libitum*. Prior to the start of all experiments, all animals were group housed. Animals were housed individually after injections and implantations. All procedures were conducted in accordance to the European Directive 2010/63/EU and were approved by the Animal Experimental Ethical Committee of Ghent University (ECD 20/21 & 22/39).

2.3. Pharmacokinetics of intraventricular cCPA administration

2.3.1. Injections and sample preparation

Animals ($n = 15$) were randomly divided over 5 timepoints post-injection (15 min, 30 min, 1 h, 2 h and 4 h) for sacrifice and sampling of blood and brain tissue. Mice were anesthetized with isoflurane (5 % at 2 l/min for induction, 2 % at 0.5 l/min for maintenance) and mounted into a stereotaxic frame (Stoelting, USA). Body temperature was monitored and kept stable using a rectal probe connected to a heating pad. A midline incision was made in the scalp to expose the skull, a hole was drilled above the left lateral ventricle and a 5 μl Hamilton Neuros syringe (Hamilton Company, USA) was inserted for intracerebroventricular (ICV) injection (coordinates: −0.3 mm AP and + 1.0 mm ML relative to bregma, −2.2 mm DV relative to dura). Mice were injected with 25 μg cCPA (dissolved in 1.25 μl DMSO) at a rate of 10 μl/min, controlled by a Quintessential Stereotaxic Injector (Stoelting, USA). A control animal was injected with vehicle solution (1.25 μl DMSO) for use as background correction in the analysis. The syringe was left in place for 3 min after which it was slowly retracted. The skin was closed with non-degradable stitches and animals were either kept under anesthesia until the selected timepoint (15 & 30 min post-injection) or placed in an individual cage and allowed to recover (1 h, 2 h & 4 h post-injection).

Animals were euthanized at the predetermined post-injection timepoint with an overdose of sodium pentobarbital (1500 mg/kg, i.p.) and blood samples (0.3–0.6 ml) were drawn *via* intracardiac puncture and collected in lithium heparin tubes. Immediately after blood collection, transcardial perfusion was performed with phosphate-buffered saline (PBS) after which the brain was isolated and rinsed with PBS. Both hippocampi were separated from the remainder of the brain (further referred to as brain samples). Hippocampus and brain samples were weighed while blood samples were centrifuged at 2000*g* for 15 min after which 50 μl of plasma was collected. Blank samples from an additional control animal, which received no injections, were spiked with a known dose of cCPA (5 μg, 200 ng and 900 ng cCPA for hippocampus, brain and blood samples respectively). Tissue and plasma samples were then processed for the extraction of cCPA and CPA for UHPLC-MS analysis. Brain tissue was vortexed and homogenized in a 1:4 mixture of mobile phase A and acetonitrile (250 μl for hippocampi, 750 μl for the remainder of the brain). Plasma samples (50 μl) were added to 250 μl of this mixture and vortexed. All samples were then centrifuged at 3000*g* for 15 min, after which supernatant was evaporated to dryness under a nitrogen stream and resuspended in 50 μl of mobile phase A. This was followed by centrifugation at 20,000*g* for 15 min, after which the supernatant was transferred to UHPLC glass vials for analysis.

2.3.2. UHPLC-MS analysis

Caged CPA and CPA were detected and quantified on a Waters Acquity® UHPLC H-class system (Waters Corporation, USA), connected to a Waters Xevo™ TQ-S triple quadrupole mass spectrometer with electrospray ionization (operated in positive ionization mode). Autosampler tray and column oven were kept at 10 °C and 60 °C, respectively. Chromatographic separation was achieved on a Waters Acquity® UPLC Peptide BEH C18 column (300 Å, 1.7 μm, 2.1 mm × 100 mm). The mobile phases consisted of 95/5 water/acetonitrile (*v*/v) containing 0.1 % formic acid (mobile phase A) and 5/95 water/acetonitrile (v/v) containing 0.1 % formic acid (mobile phase B); the flow rate was set to 0.5 ml/min. A 5 μl aliquot from each sample was injected. The gradient program for cCPA started with 65 % of mobile phase A for 1 min, followed by a linear gradient to 20 % of mobile phase A for 4 min; a 2 min equilibration period was included, before starting conditions were applied. The retention time of cCPA was around 2.9 min. For CPA, the gradient started with 90 % of mobile phase A for 1 min, followed by a linear gradient to 20 % of mobile phase A for 6.5 min and a 5 min equilibration period, before starting conditions were again applied. The retention time of CPA was around 1.5 min.

An optimized capillary voltage of 4.00 kV, a cone voltage of 40 V, and a source offset of 80 V were used. Acquisition was done in the MRM mode: the precursor ion for cCPA was *m/z* 609.29 with product ion *m/z* 477.29 (15 eV), while the precursor ion for CPA was *m/z* 336.16 with product ion *m/z* 204.14 (25 eV). Limits of detection were determined as analyte mass for which the signal-to-noise ratio was >3. Values indicate limits of detection for cCPA in 2×10^{-3} nanograms per milligram wet weight for tissue samples and 1×10^{-3} nanograms per microliter for plasma samples. Limits of detection for CPA were in 1×10^{-4} nanograms per milligram wet weight and 1×10^{-5} nanograms per microliter for tissue and plasma samples respectively.

2.4. Evoked potential recordings with CPA & cCPA administration

2.4.1. Stereotaxic surgeries

In a terminal experiment, healthy mice were anesthetized and mounted into a stereotaxic frame as described above (section 2.3.1). After exposing the skull, holes were drilled for ICV injection and placement of electrodes. A 5 μl Hamilton Neuros syringe (Hamilton Company, USA) was inserted in the right lateral ventricle (coordinates: −0.3 mm AP and + 1.0 mm ML relative to bregma, −2.2 mm DV relative to dura). On the contralateral side, a bipolar recording electrode (200 μm tip separation) was lowered into the DG (coordinates: −2.0 mm AP and + 1.3 mm ML relative to bregma, −2.0 mm DV relative to dura) and a bipolar stimulation electrode (500 μm tip separation) into the perforant path (coordinates: −3.7 mm AP and + 2.0 mm ML relative to bregma, −1.5 mm DV relative to dura). Bipolar electrodes were fabricated from two twisted polyimide-coated stainless-steel wires of 70 μm (recording) and 120 μm (stimulation) diameter (California Fine Wire,

USA). An epidural screw electrode (stainless steel, 1.57 mm diameter, Bilaney Consultants, Germany) was placed in the frontal bone as ground/reference electrode. For experiments with illumination, the recording electrode was combined with a multi-mode optical fiber (400 μm core diameter, 0.50 NA, FP400URT, Thorlabs, Germany) into an optrode, the distal contact of the bipolar electrode protruding 300 μm from the tip of the optical fiber. Prior to insertion into the brain, light output was measured at the tip of the optical fiber using a photodiode power sensor (S120VC coupled to PM100A, Thorlabs, Germany) and set to the desired intensity. The position of the recording and stimulation electrodes was adjusted using electrophysiological feedback until optimal evoked potential (EP) waveforms were acquired. Recordings were started once all electrodes and the syringe were set in place. After conclusion of the EP recordings, animals were euthanized with an overdose of sodium pentobarbital (1500 mg/kg, i.p.).

2.4.2. Recording protocol

Recording of hippocampal field potentials was done using a custom MATLAB-based script (MathWorks, USA), controlling a USB-6211 NI-DAQ card (National Instruments, USA) for data acquisition and stimulation. Field potentials were high-pass filtered at 0.1 Hz, amplified 248 times and digitized at 10 kHz with a 16-bit resolution (input range of ±10 V). Recordings were stored on a PC for off-line analysis. Every 10 s, a 6-s sweep of electroencephalography (EEG) was recorded. To record EPs, the perforant path was stimulated at the start of every sweep by delivering biphasic square-wave pulses (200 μs per phase) through the stimulation electrode, generated by a constant current linear stimulus isolator (Digitimer, UK). Input-output (I/O) curves were constructed by stimulating every 10 s at increasing current intensities (50–500 μA in increments of 50 μA, 500–1000 μA in increments of 100 μA), repeated four times. The intensity evoking about 50 % of the maximal PS amplitude on the averaged I/O curve was determined and used as stimulation intensity for the subsequent EP recordings.

In a first batch of animals, the effect of two ICV administered CPA doses was studied, based on dose-ranges reported in literature [43]. After at least 10 min of baseline EP recording, a 5 μl solution was injected in the lateral ventricle at a rate of 10 μl/min with the Hamilton syringe controlled by a Quintessential Stereotaxic Injector (Stoelting, USA). Animals received either 0.25 μg CPA ($n = 5$), 1.25 μg CPA ($n = 7$) or vehicle (2.5 % DMSO in 5 μl saline, $n = 4$). Recordings were continued for at least 60 min after injection.

In a second batch of animals, cCPA was administered ICV either with (cCPA-light, $n = 8$) or without illumination (cCPA-dark, n = 7) of the dorsal DG. In the cCPA-light group, the optrode implanted in the hippocampus was connected to a 405 nm light-emitting diode (M405FP1, Thorlabs, Germany) *via* a patch cable (M98L01, Thorlabs, Germany). The illumination protocol consisted of 100 ms light pulses at a frequency of 0.1 Hz (1 % duty cycle) with an intensity of 8 mW (63.7 mW/mm^2 at optical fiber tip). After baseline EP recordings, 25 μg cCPA (dissolved in 1.25 μl DMSO) was injected ICV at a rate of 10 μl/min. Recordings were continued for at least 60 min, with a 20-min illumination period applied 10 min after injection. Directly after conclusion of the recording, the optrode was removed from the brain and its light output was measured. In 2 out of 8 mice, the output had decreased by more than 50 % of the starting value (due to damage to the fiber or coverage of optical fiber tip by blood) and thus recordings were excluded. In the cCPA-dark group, baseline EP recordings were followed by injection of 25 μg cCPA and at least 60 min of recording after injection without illumination.

2.5. cCPA administration in the IHKA model

2.5.1. IHKA injections

Mice ($n = 12$) received unilateral hippocampal injections of kainic acid (KA) for the induction of status epilepticus. Animals were anesthetized and placed into the stereotaxic frame as described above (section 2.3.1). After exposing the skull, a hole was drilled for injection of KA into the right hippocampus (coordinates: −2.0 mm AP and + 1.5 mm ML relative to bregma). A glass capillary loaded with KA solution (4 mg/ml KA in saline) was lowered into the dorsal hippocampus (−1.8 mm DV relative to dura) and 50 nl was infused at a rate of 100 nl/min using a Nanoliter injector system (World Precision Instruments, USA). The capillary was left in place for 5 min after injection and then slowly retracted to prevent backflow. Afterwards, the skin was closed with non-degradable stitches and animals were observed after waking up from anesthesia for signs of status epilepticus.

2.5.2. Implantations

Three weeks after KA injection, mice underwent a second stereotaxic surgery for implantation of an optrode in the right hippocampus and a guide cannula above the left lateral ventricle. The optrodes consisted of a bipolar electrode (polyimide-coated stainless-steel wire, California Fine Wire, USA) combined with a multi-mode optical fiber (400 μm core diameter, 0.50 NA, FP400URT, Thorlabs, Germany) and had an average light transmission of 82 ± 2 % compared to the output measured at the tip of the patch cable. Animals were anesthetized and placed into the stereotaxic frame as described above (section 2.3.1). Holes were drilled for insertion of an optrode in the injected hippocampus (coordinates: −2.0 mm AP and + 1.5 mm ML relative to bregma, −2.0 mm DV relative to dura) and implantation of a guide cannula (C316G-SPC, Bilaney Consultants, Germany) above the lateral ventricle on the contralateral site (coordinates: −0.3 mm AP and + 1.0 mm ML relative to bregma, −0.8 mm DV relative to dura). Additional burr holes were made for the placement of 2 epidural screw electrodes and 2 anchor screws. One epidural electrode was placed over parietal cortex contralateral to the optrode for recording of cortical EEG, the other epidural electrode was placed over frontal cortex to serve as ground/reference electrode. Electrode leads were attached to a connector and assembled into a headcap together with the optrode and guide cannula using dental acrylic cement.

Mice were allowed to recover from surgery for at least one week. Following recovery, they were handled and habituated to the procedure of ICV injection, which consisted of one researcher restraining the awake animal and immobilizing the head while a second researcher inserted a Hamilton syringe through the guide cannula to manually inject vehicle solution (1.25 μl DMSO) in the ventricle (−2.2 mm DV relative to dura). The syringe was kept in place for 1 min after which it was slowly retracted to prevent backflow.

2.5.3. EEG recordings in the IHKA model with cCPA administration

After implantation and habituation, mice were connected to an EEG setup *via* their headcap. This setup consisted of a unity gain preamplifier, a 6-channel cable, a commutator and 512× amplifier, leading to a USB-6259 NI-DAQ card (National Instruments, USA). Signals were high-pass filtered at 0.15 Hz and digitized at 2 kHz (16-bit resolution, input range ± 10 V). Recordings were controlled *via* custom made MATLAB (MathWorks, USA) software and stored on a PC for off-line analysis. Baseline EEG was recorded for 4 h and evaluated for the presence of electrographic hippocampal seizures. Animals that displayed clear seizures were selected for a cross-over study (7 out of 12 animals).

The cross-over design consisted of 3 treatments: ICV administration of 25 μg cCPA without illumination (cCPA-dark), 25 μg cCPA with illumination (cCPA-light) and vehicle (1.25 μl DMSO) with illumination (vehicle-light). Animals were randomly assigned to 1 of 3 sequences to receive all 3 treatments, with a 2-day washout in between each treatment. On the day of the treatment, animals were connected to the EEG setup and at least 2 h of baseline EEG was recorded. Animals were disconnected for ICV injection and afterwards immediately returned to the setup to continue EEG recording for at least 4 h. For treatments including illumination, animals were also connected with the implanted optrode to a 405 nm laser diode (LP405-MF300, Thorlabs, Germany) *via* a patch cable (M127L01, Thorlabs, Germany). Illumination was performed for a period of 2 h immediately after injection and consisted of 100 ms light pulses with an intensity of 50 mW (397.9 mW/mm^2, output measured at the patch cable tip) at a frequency of 0.1 Hz. Six out of 7 animals underwent all 3 treatments, one animal lost its headcap after the first treatment with

cCPA-dark. Of those 6, the EEG of one animal during vehicle treatment could not be analyzed due to a bad connection to the EEG setup.

In a subset of animals ($n = 3$), additional recordings were performed to control for possible effects of the photocage DEACM, which is released upon photo-uncaging of cCPA. After recording baseline EEG for at least 2 h, animals were injected with DEACM solution (10.14 μg in 1.25 μl DMSO), equimolar to the cCPA solution used, after which EEG recordings were continued for at least 4 h.

2.6. Behavioral testing

Healthy mice ($n = 6$) were implanted with an optrode and a guide cannula and habituated to ICV injections following the same procedures as described above (section 2.5.2).

The effects of CPA and cCPA administration on locomotor activity were tested with the accelerating rotarod test [44]. Mice were placed on a rotarod apparatus (Mouse RotaRod, Ugo Basile, Italy), set to accelerate from 4 rpm to 40 rpm over 300 s and the time to the end of each trial was recorded. The trial ended when the animal either fell off the rotarod, completed 2 full rotations when clinging on to the rod or when it ran for 300 s. Animals first underwent training for 3 consecutive days, consisting of 10 rotarod trials separated by a 3-min rest period each day. This allowed the animals to learn the task and reach a plateau in their performance by the third day of training [45]. After completion of the training, animals were tested on the rotarod after administration of 4 different treatments in the following order: ICV administration of vehicle (1.25 μl DMSO) with illumination, 25 μg cCPA without illumination (cCPA-dark), 25 μg cCPA with illumination (cCPA-light) and CPA (1 μg) with illumination. Each treatment was separated by 2 days of wash-out.

On the day of treatment, animals were connected to the EEG setup *via* their headcap and one hour of baseline EEG was recorded. Afterwards, animals were disconnected for ICV injection and immediately returned to the setup to continue EEG recording for 30 min. For treatments including illumination, animals were also connected to the 405 nm laser diode and illumination (100 ms pulses at 0.1 Hz, 50 mW) was performed during the 30 min recording after injection. After conclusion of these recordings, animals were disconnected and placed on the rotarod to perform the accelerating rotarod test.

2.7. Histological verification

The correct placement of the guide cannula and optrode was histologically verified in implanted animals after conclusion of the experiments (**Supplementary Fig. 1**). Mice were anesthetized and 0.5 μl of Evans Blue dye solution (1 % *w/v* in saline) was injected through the guide canula prior to euthanasia with an overdose of sodium pentobarbital (1500 mg/kg, i.p.). Transcardial perfusions were performed with PBS followed by 4 % paraformaldehyde solution. Brains were isolated, cryoprotected with 30 % sucrose solution and snap-frozen in isopentane. Coronal sections of 40 μm thickness were made on a cryostat (CM1950, Leica, Germany) and stained with cresyl violet (0.1 % *w/v*).

2.8. Data analysis

2.8.1. UHPLC-MS data and pharmacokinetic analysis

Concentrations of cCPA and CPA detected in the samples representing the different timepoints were calculated based on values obtained from UHPLC-MS analysis of the samples spiked with cCPA and a solution with a known concentration of CPA. Data from the samples of the control animal injected with vehicle solution was used for background subtraction. A correction factor was applied for the proportion of CPA released from cCPA during the sample preparation, extraction and UHPLC-MS analysis procedures. Concentrations of cCPA and CPA are expressed as ng/mg for hippocampus and brain samples and as ng/μl for blood samples. For conversion to molar concentration, a density of 1.04 g/ml for mouse brain tissue was used [46]. Data was averaged per timepoint ($n = 3$) for each tissue and non-compartmental analysis was used to determine the following pharmacokinetic parameters: time of maximal concentration (T_{max}), maximal concentration (C_{max}), the terminal elimination rate constant (K_e) and the terminal half-life ($T_{½}$). K_e values were calculated as the slope from the regression line fitted to the log concentrations of the final 3 timepoints. $T_{½}$ was calculated using the formula $T_{½} = \ln(2)/ K_e$. One blood sample collected at timepoint 60 min post-injection displayed an extreme value for the cCPA concentration compared to all other samples (> 1.5 IQR above Q3) and was excluded as outlier [47].

2.8.2. Evoked potentials

Hippocampal EPs were analyzed using custom MATLAB (MathWorks, USA) software, measuring the field excitatory post-synaptic potential (fEPSP) amplitude and population spike (PS) amplitude for each evoked response. The fEPSP amplitude was calculated as the maximum value of the fEPSP peak. The PS amplitude was calculated as the distance between the negative peak of the PS and the line connecting the positive peaks before and after the PS (Fig. 2 **B**). Values were normalized to the mean of baseline and averaged per 5 min.

2.8.3. EEG power

Power spectral analysis of all recorded EEG data was performed using custom scripts in Python (v3.8.5, Python Software Foundation). The differential EEG signals derived from the bipolar electrode in the hippocampus were high-pass filtered at 1 Hz (1st-order Butterworth) and segmented into 1-s epochs with 50 % overlap. These segments were windowed (Blackmann-Harris) after which the Fast Fourier algorithm was used to compute the power spectra, divided over the following frequency bands: total power (1–100 Hz), delta (1–3 Hz), theta (4–12 Hz), beta (13–30 Hz), gamma (31–100 Hz). For subsequent analyses, frequencies around 50 Hz (48–52 Hz) were excluded to avoid power line interference. Power values were log-transformed into decibels (10*log10), the average power per Hz was taken for each frequency band and the difference in power to baseline was calculated.

For the EP recordings (section 2.4), power spectra were obtained from the last 5 s of each 6-s sweep and averaged per 5 min. From 1 recording in the high dose group, EEG power could not be analyzed due to incomplete EEG-sweeps. For the EEG recordings in the IHKA model (section 2.5), the average power spectra were calculated from 5 interictal 1-min segments which were randomly selected from the 2-h baseline period and from the 2-h period after injection. For the EEG recordings from the rotarod test (section 2.6), power spectra were calculated from the last 20 min of the baseline recording and the 20-min segment from minute 10 to minute 30 after injection.

2.8.4. Seizure frequency

Seizures were annotated and counted by researchers (J.S., M.D., T. M.) blinded to the treatment. They were defined as a repetitive pattern (> 2 Hz) of high-amplitude EEG spikes (>2× amplitude of background EEG) that lasted a minimum of 7 s and were separated by at least 7 s from a previous seizure. The seizure frequency was calculated per 30 min and normalized to the 2-h baseline period.

2.8.5. Rotarod

The latency to fall, expressed in seconds, was recorded for each trial on the accelerating rotarod, with a maximum latency of 300 s if animals completed the trial without falling. One trial (one animal with vehicle treatment) where the animal turned around on the rotarod and started walking backwards was excluded.

2.9. Statistical analysis

Statistical analyses were performed using SPSS Statistics (version 29.0, IBM Corp., USA). For the acute EP recordings, the effects of CPA and cCPA administration were compared between the vehicle, low dose CPA and high dose CPA groups and between the cCPA-light and cCPA-dark

groups, respectively. The effects over time on EP parameters and EEG power were evaluated using a restricted maximum likelihood (REML) linear mixed effects model with either fEPSP amplitude, PS amplitude or EEG power as dependent variable, group, time and group by time interaction as fixed factors and animal ID as random factor. The first-order autoregressive model was used as covariance structure to account for repeated measures over time. Fisher's Least Significant Difference (LSD) test was used for *post-hoc* comparison of timepoints between groups.

For the EEG recordings in the IHKA model, the average seizure frequency and interictal EEG power of the 2-h period after injection were compared using a REML linear mixed effects model with either seizure frequency or EEG power as dependent variable, treatment condition and treatment period (1st, 2nd or 3rd injection) as fixed factors and animal ID as random factor. Compound symmetry was used as covariance structure and Fisher's LSD for *post-hoc* comparison.

For the data from the rotarod test, the performance on the accelerating rotarod and EEG power were compared between conditions. A REML linear mixed effects model was constructed with either latency to fall or EEG power as dependent variable, treatment condition as fixed factor, animal ID as random factor, using compound symmetry as covariance structure and Fisher's LSD for *post-hoc* comparison.

For all statistical analyses, a two-tailed p-value <0.05 was set for statistical significance. Group values are reported and plotted as means ± standard error of the mean.

3. Results

3.1. Concentrations of cCPA & CPA after ICV administration

In order to investigate the concentrations achieved after ICV administration of a 25 μg dose of cCPA and explore its pharmacokinetic profile and stability, cCPA and CPA concentrations were measured in brain tissue and blood at 5 timepoints post-injection: 15 min, 30 min, 1 h, 2 h and 4 h (Fig. 3).

The highest concentrations of cCPA were detected in the hippocampus, with a maximal concentration (C_{max}) of 131.88 ± 16.18 ng/mg (= 208.34 ± 25.56 μM) 15 min post-injection. The cCPA concentrations in the hippocampus followed an immediate, slow decline with a half-life ($T_{½}$) of 3.6 h (elimination rate constant K_e = 0.19/h). The cCPA concentrations measured in the brain samples were 65–100 times lower, with C_{max} = 1.35 ± 0.10 ng/mg (= 2.14 ± 0.16 μM) at T_{max} = 30 min. These concentrations started to decline after the 60 min post-injection timepoint with a similar rate as in the hippocampus ($T_{½}$ = 3.2 h, K_e = 0.22/h). Low concentrations of cCPA were also detected in the blood already from the earliest timepoint (T_{max} = 15 min), where they reached a C_{max} = 1.20 ± 0.35 ng/μl (= 1.96 ± 0.58 μM). These displayed a steep initial decline and a comparatively shorter terminal half-life of 1.2 h (K_e = 0.57/h). No CPA was measured in hippocampus and blood samples after correction for CPA-release caused by the analysis procedures In the brain samples, CPA concentrations were measured at 185–470 times lower concentrations than those of cCPA, with C_{max} = 0.0039 ± 0.0002 ng/mg (= 11.26 ± 0.51 nM) at T_{max} = 15 min.

3.2. Effects of A_1R activation on hippocampal electrophysiology

We measured hippocampal EPs in healthy mice under anesthesia to test whether local photo-uncaging of cCPA can lead to sufficient levels of CPA release to induce A_1R signaling and reduce neurotransmission and excitability in hippocampal neurons. First, we validated the expected decrease in EP parameters upon ICV administration of CPA. Then, we examined whether a similar reduction could be achieved using ICV administration of cCPA combined with local illumination.

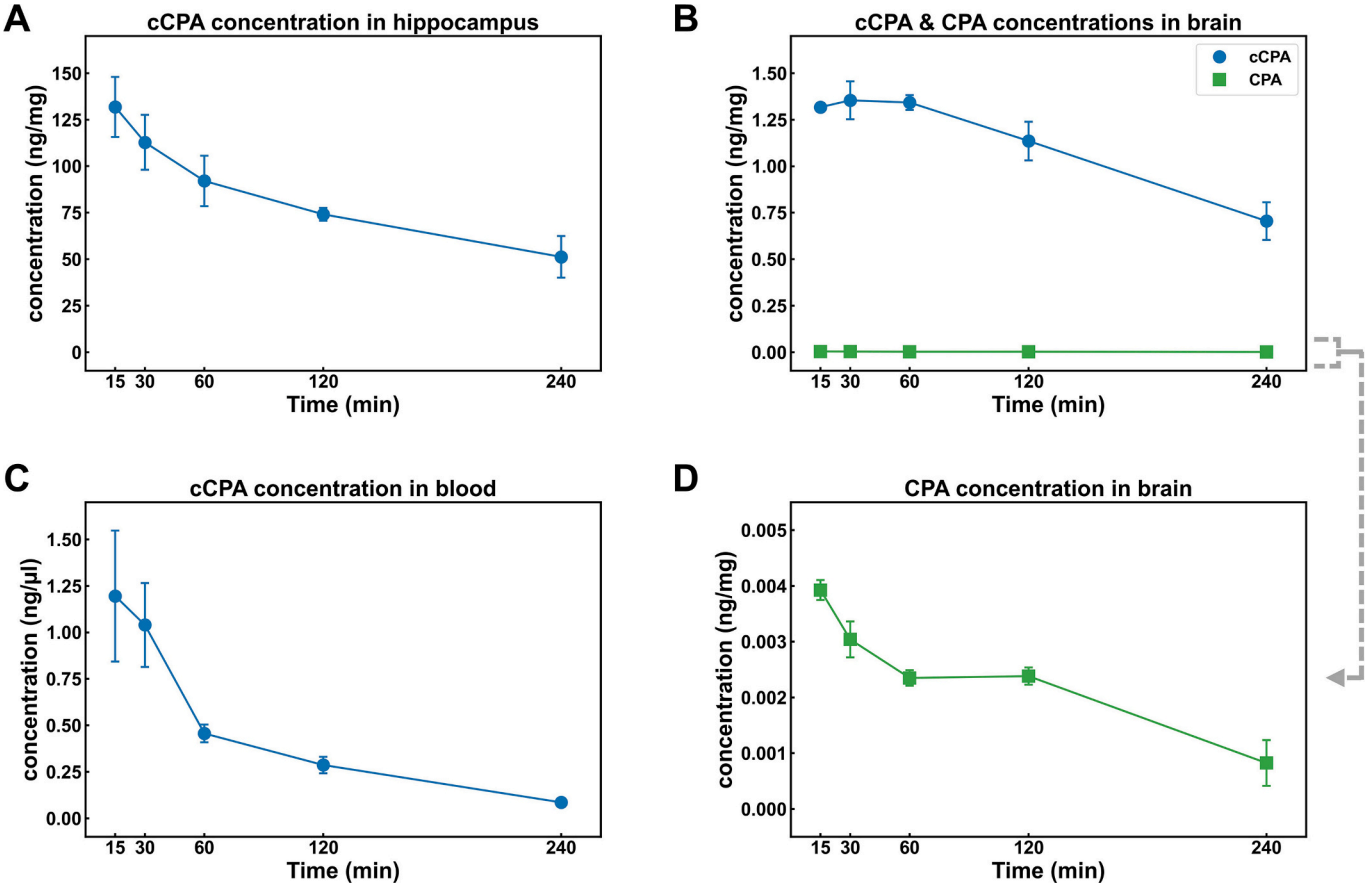

Fig. 3. Concentrations of cCPA and CPA plotted over time (**A**) in the hippocampus, (**B**) in brain and (**C**) in blood. Mice received an intracerebroventricular injection of 25 μg cCPA after which concentrations of cCPA and CPA were measured after 15 min, 30 min, 1 h, 2 h and 4 h. (**D**) Small quantities of CPA were found only in the brain samples, depicted in a separate graph below (with adjusted scale for the y-axis). $N = 3$ for all data points except for the blood concentrations at t_{60}, where $n = 2$.

3.2.1. Dose-dependent suppression of EPs after ICV administration of CPA

Changes in EP parameters and EEG power were studied after ICV injection of two doses of CPA: 0.25 μg (low dose, $n = 5$) and 1.25 μg (high dose, $n = 7$). Three out of 7 animals that received the high dose of CPA died within 20 min after injection, resulting in 4 complete recordings. Injection of CPA resulted in a dose-dependent decrease in fEPSP and PS amplitudes (Fig. 4 **B**—**C**). The PS was most sensitive to effects of CPA administration, reaching a minimum of 62 ± 13 % of

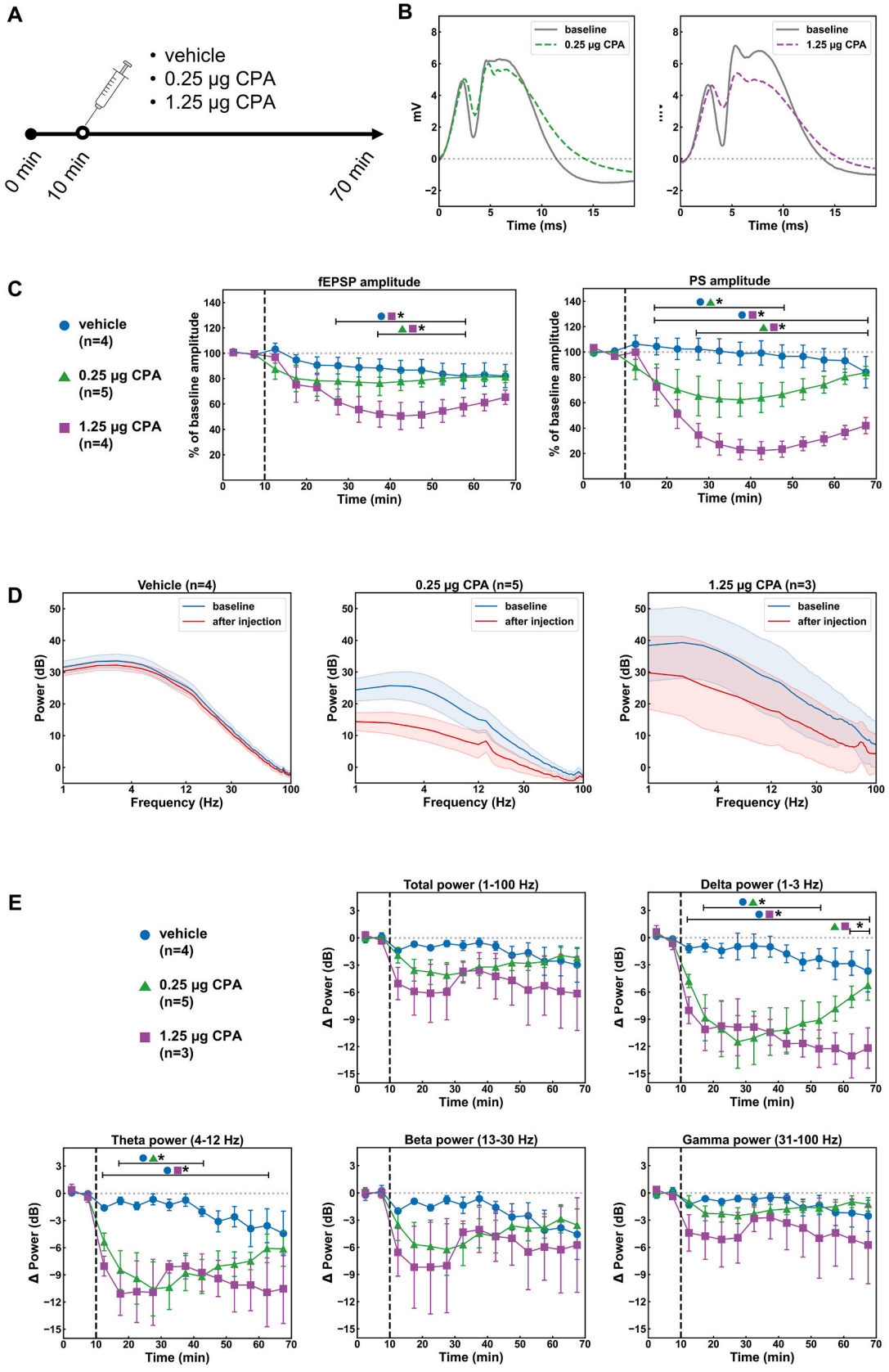

(caption on next page)

Fig. 4. Effects of intracerebroventricular (ICV) injection of CPA on hippocampal evoked potentials (EPs) and electroencephalography (EEG) power. (**A**) Recording protocol: after 10 min of baseline EP recording, animals received an ICV injection of 0.25 μg CPA ($n = 5$), 1.25 μg CPA ($n = 4$) or vehicle (2.5 % DMSO, n = 4) and recordings were continued for 60 min. (**B**) Example traces of EPs recorded before (solid line) and 30 min after (dashed line) administration of both doses of CPA (left: 0.25 μg CPA; right: 1.25 μg CPA). (**C**) Dose-dependent effects of CPA on field excitatory post-synaptic potential (fEPSP) and population spike (PS) amplitudes over time. Dashed line indicates time of injection. * indicates timepoints where groups (as indicated by the symbols) significantly differ from each other with $p < 0.05$. (**D**) EEG power spectra before (0–10 min, blue) and after (20–30 min, red) ICV injection of vehicle (n = 4, left), 0.25 μg CPA (n = 5, middle) and 1.25 μg CPA (n = 4, right). (**E**) Change over time in EEG power compared to baseline in the different frequency bands (total power:1–100 Hz, delta power:1–3 Hz, theta power: 4–12 Hz, beta power: 13–30 Hz, gamma power: 31–100 Hz). Dashed line indicates time of injection. * indicates timepoints where groups (as indicated by the symbols) significantly differ from each other with $p < 0.05$. (For interpretation of the references to colour in this figure legend, the reader is referred to the web version of this article.)

baseline levels in the low dose group ($n = 5$) and a minimum of 22 ± 7 % in the high dose group ($n = 4$) between 30 and 35 min after injection. Respectively, fEPSP amplitudes reached minima of 76 ± 10 % and 51 ± 11 %. For the PS amplitude, there was a significant effect of the group factor ($F = 12.085$, $p = 0.001$) with both the low and high dose groups significantly differing from the vehicle group starting 10 min after injection, and with a significant difference between the two doses starting 20 min after injection. For the fEPSP amplitude, the effect of the group factor was near statistically significance ($F = 3.677$, $p = 0.053$) and the high dose group reached a significant difference from vehicle 20 min after injection and from the low dose group 30 min after injection in *post-hoc* testing. Spectral analysis of hippocampal EEG also displayed a dose-dependent decrease in EEG power (Fig. 4 **D-E**). The average total EEG power (1–100 Hz) was reduced with 4.1 ± 1.4 dB from baseline in the low dose group ($n = 5$) and 6.1 ± 3.2 dB in the high dose group ($n = 3$) between 10 and 20 min post-injection. Mainly the lower frequency bands were affected by CPA administration. LMM analysis revealed a significant effect of group for the delta band ($F = 9.022$, $p = 0.004$) and the theta band ($F = 5.946$, $p = 0.018$), where both doses achieved significant reductions in power compared to vehicle, while the beta band ($F = 0.858$, $p = 0.452$) and gamma band ($F = 1.144$, $p = 0.358$) showed no significant differences.

3.2.2. Suppression of EPs through photo-uncaging of cCPA

Next, EP recordings were conducted in combination with ICV injection of 25 μg of cCPA. One group of animals received pulsed 405 nm illumination at the DG (cCPA-light, $n = 6$) and was compared to a control group without illumination (cCPA-dark, $n = 7$). No animals died after injection of cCPA in either group. In the cCPA-dark group no significant effects of cCPA administration could be detected. However, in the cCPA-light group there was a clear reduction in fEPSP amplitude and PS amplitude (Fig. 5 **B—C**). After 20 min of pulsed illumination, the PS amplitude and fEPSP amplitude were reduced to minima of 46 ± 15 % and 80 ± 9 % of baseline, respectively. LMM analysis yielded a significant effect for the group factor for both EP parameters (PS amplitude: $F = 5.345$; $p = 0.034$; fEPSP amplitude: $F = 7.009$, $p = 0.018$). Photo-releasing CPA also caused a small decrease in EEG power (Fig. 5 **D-E**). Ten minutes after the start of illumination, average total EEG power (1–100 Hz) was reduced with 3.0 ± 1.1 dB from baseline in the cCPA-light group. The effects were visible across all frequency bands and confirmed by LMM analysis, with significant differences between groups for each band (total power: $F = 12.432$, $p = 0.002$; delta: $F = 16.177$, $p < 0.001$; theta: $F = 11.559$, $p = 0.002$; beta: $F = 14.693$, $p < 0.001$; gamma: $F = 21.360$, $p < 0.001$).

3.3. Suppression of seizures through photopharmacological A_1R activation

After confirming a potent reduction in hippocampal neurotransmission induced by local photo-release of CPA in the acute experiments, we evaluated the seizure-suppressing effects of administering the same ICV dose of cCPA (25 μg) combined with pulsed hippocampal illumination (100 ms pulses of 50 mW 405 nm light at 0.1 Hz) in epileptic IHKA mice.

Based on the presence of clear electrographic seizures during baseline EEG recording, 7 out of 12 animals were selected for inclusion. Animals received 3 treatments in randomized order: vehicle, cCPA-dark and cCPA-light. Administration of cCPA combined with illumination led to a strong decrease in seizure frequency compared to baseline (23 ± 16 % of baseline), where in 3 animals seizures were completely absent during the 2 h illumination period (Fig. 6 **B—C**). The other conditions had no effect on seizures compared (vehicle: 96 ± 5 % of baseline; cCPA-dark: 92 ± 10 % of baseline). LMM analysis confirmed that seizure frequency indeed was different between conditions ($F = 10.133$, $p = 0.005$), independent of treatment period (1st, 2nd or 3rd injection), with a significantly lower amount of seizures in the cCPA-light condition compared to vehicle ($p = 0.006$) and cCPA-dark ($p = 0.003$) conditions. No statistical differences between vehicle and cCPA-dark were observed. While there was an initial drop in seizure frequency in all 3 conditions immediately after the injections, the course of seizure frequency plotted over time displayed a stable decrease of seizure activity only in the cCPA-light condition during the 2-h illumination period. In the following 2 h after illumination, seizure frequencies started increasing back up to around 50 % of baseline (Fig. 6 **D**). Spectral power analysis of the interictal EEG also showed these differences between conditions, although less pronounced. The average power spectra of the vehicle and cCPA-dark conditions did not differ from baseline, while the average total power (1–100 Hz) in the cCPA-light condition was reduced with 4.1 ± 2.3 dB relative to baseline (Fig. 6 ***E*-F**). The main effects were found in the higher frequency ranges. Power in the theta, beta and gamma bands showed a trend towards reduction in the cCPA-light condition (theta: −5.6 ± 3.7 dB; beta: −5.2 ± 3.3 dB; gamma: −4.1 ± 2.0 dB), but no statistically significant difference was reached (delta: $F = 0.232$, $p = 0.797$; theta: $F = 1.854$, $p = 0.202$; beta: $F = 1.607$, $p = 0.245$; gamma: $F = 3.302$, $p = 0.076$).

Control injections of the photocage DEACM were performed in 3 animals after the cross-over trial. Neither seizure frequency (102 ± 5 % of baseline) nor the EEG power spectrum were affected by DEACM compared to baseline (**Supplementary Fig. 2**).

3.4. Side effects of CPA & cCPA on locomotor activity

To confirm that ICV injection of cCPA was not associated with the typical sedative effects of CPA, we compared the effects of cCPA and CPA administration on locomotor performance in the accelerating rotarod test and on hippocampal EEG. In addition, we evaluated possible sedative effects of photo-releasing CPA by local illumination in dentate gyrus.

Intracerebroventricular injection of 1 μg of CPA caused strong sedative effects with a clear reduction in rotarod performance. Half of the animals were too sedated after injection to perform the rotarod trial, while the other half had a notably reduced latency to fall compared to the other conditions, resulting in an overall average latency to fall of 75 ± 35 s. The latency to fall in cCPA-dark conditions (245 ± 25 s) was comparable to vehicle-light conditions (230 ± 26 s). Variable results were seen in cCPA-light conditions: 3 animals performed equally well as in the vehicle-light and cCPA-dark conditions, 1 animal had a decreased latency and 2 animals were too sedated to perform the rotarod trial, resulting in an overall average latency to fall of 168 ± 54 s. Statistical analysis confirmed a significant effect for the condition factor ($F = 6.958$, $p = 0.004$). Only performance after the CPA treatment was

significantly reduced compared to vehicle ($p = 0.004$), cCPA-dark ($p < 0.001$) and cCPA-light ($p = 0.035$) treatments (Fig. 7 **B**). Spectral analysis showed that impaired locomotor performances in both the cCPA-light and CPA conditions were associated with reductions in EEG power recorded immediately before the rotarod trials. Similarly to the rotarod results, the average power spectra after vehicle and cCPA-dark

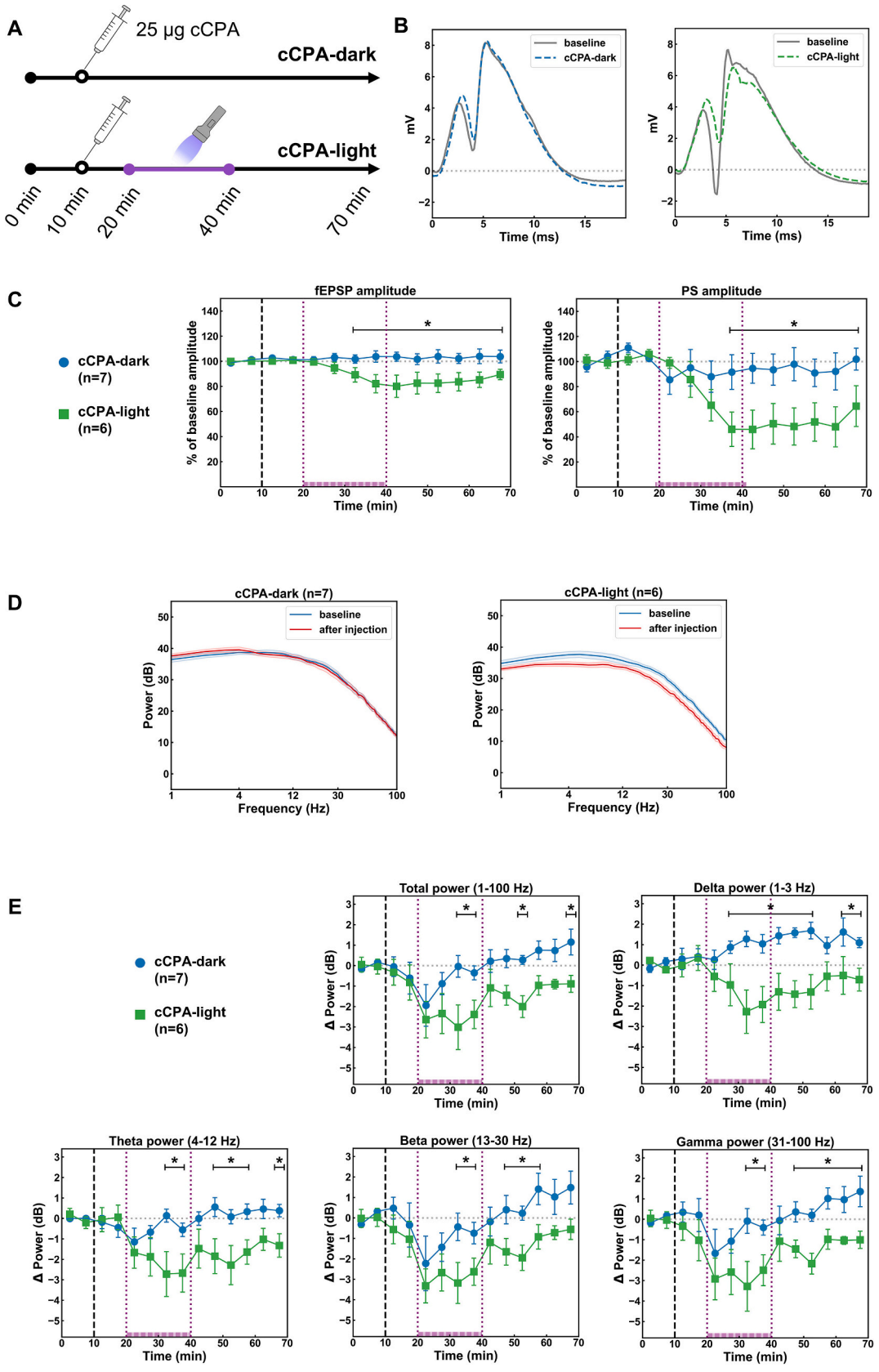

(caption on next page)

Fig. 5. Effects of CPA photo-releasing after ICV administration of cCPA on hippocampal evoked potentials (EPs) and electroencephalography (EEG) power. (**A**) Recording protocol: after 10 min of baseline EP recording, animals received an ICV injection of 25 μg cCPA and recordings were continued for 60 min with (cCPA-light, $n = 6$) and without (cCPA-dark, $n = 7$) 405 nm illumination. Pulsed illumination was started 10 min after injection and applied for 20 min. (**B**) Example traces of EPs recorded before (solid line) and 30 min after (dashed line) administration of cCPA without (left) and with (right) illumination. (**C**) Effects of photo-releasing CPA on field excitatory post-synaptic potential (fEPSP) and population spike (PS) amplitudes over time. Dashed line indicates time of injection, dotted lines indicate start and end of illumination in the cCPA-light group. * indicates timepoints where cCPA-light significantly differs from cCPA-dark with $p < 0.05$. (**D**) EEG power spectra before (0–10 min, blue) and after (30–40 min, red) ICV injection of cCPA without (left, n = 7) and with (right, n = 6) illumination. (**E**) Change over time in EEG power compared to baseline in the different frequency bands (total power: 1–100 Hz, delta power: 1–3 Hz, theta power: 4–12 Hz, beta power: 13–30 Hz, gamma power: 31–100 Hz). Dashed line indicates time of injection, dotted lines indicate start and end of illumination in the cCPA-light group. * indicates timepoints where cCPA-light significantly differs from cCPA-dark with $p < 0.05$. (For interpretation of the references to colour in this figure legend, the reader is referred to the web version of this article.)

treatments did not differ. The cCPA-light conditions were associated with an average reduction of total EEG power (1–100 Hz) of 6.2 ± 3.5 dB relative to baseline, while CPA treatment led to a decrease of 8.0 ± 3.0 dB (Fig. 7 **C**—**D**). The effects on EEG power did not reach statistical significance in the LMM in any of the frequency bands (delta: $F = 1.093$, $p = 0.383$; theta: $F = 3.142$, $p = 0.57$; beta: $F = 2.596$, $p = 0.091$; gamma: $F = 2.838$, $p = 0.073$).

4. Discussion

This *in vivo* study is the first to demonstrate that a photocaged A_1R agonist can be used for light-mediated control of neuronal excitability. Intracerebroventricular administration of cCPA in combination with local 405 nm illumination led to a reduction of both the fEPSP and the PS amplitude, similar to what was observed after direct ICV administration of CPA, indicating successful photo-release of CPA. Furthermore, administration of cCPA in the absence of illumination did not affect EPs, confirming that the photocage renders the agonist inactive at these effective concentrations. This was further supported by the finding that a 25 μg dose of cCPA could safely be administered, while ICV administration of 1.25 μg CPA (3.7 nmol) in mice lead to 43 % mortality. While previous studies did not report any deaths with ICV administration of similar CPA doses in conscious mice [43], diffusion of CPA into the respiratory center possible caused lethal apnea in combination with isoflurane anesthesia [48]. Although a more than 10-fold higher molar dose of cCPA (25 μg cCPA = 41.1 nmol) was used, no animals died under anesthesia after injection of cCPA.

These findings are in accordance with our previous study where we demonstrated in an *ex vivo* setting the potential of cCPA to release CPA and achieve light-controlled activation of adenosine A_1 receptors, resulting in a reduction of hippocampal excitability due to the well-known pre- and postsynaptic G_i-mediated effects [36]. Achieving these effects *in vivo* proved more difficult due to the differences in experimental settings between the previously described *ex vivo* MEA recordings and the current *in vivo* EP recordings. In the former, thanks to the 2-dimensional configuration of the brain slices bathed in solution containing cCPA, a single light flash sufficed to elicit changes in EPs. In the current *in vivo* setting, it was more difficult to reach sufficient levels of photo-uncaging in the intact brain. The brain volume that can be illuminated *in vivo* is limited due to high attenuation of light in tissue, which is known as one of the major challenges for the application of photopharmacology *in vivo* [49]. Additionally, only a fraction of the injected cCPA is able to reach the hippocampus where it is then available for photo-uncaging. With injections of 25 μg cCPA, we now measured a maximal hippocampal concentration of 131.88 ng/mg (= 208 μM), while the concentrations in the rest of the brain were 65–100 times lower. It is indeed known that ICV administration is an effective way to ensure delivery of compounds to the brain, especially in periventricular regions such as the hippocampus [50]. Compounds diffused in the CSF are also known to be cleared through drainage into the venous sinuses. Accordingly, cCPA was also detected in the blood, albeit at relatively low amounts. Of the amount of cCPA that reached the hippocampus, we estimate that only a miniscule proportion is photo-uncaged. Based on our previous *ex vivo* results with CPA and other studies evaluating the effects of CPA on hippocampal slices, it is known that a 50 % reduction in fEPSP amplitude is reached with ±12–20 nM concentrations of CPA [51–53]. Considering the 20 % reduction in fEPSP amplitude we observed in this study with cCPA *in vivo*, we estimate the concentration of CPA that was locally released to be in the low nanomolar range. This amounts to less than 10^{-4} times the local concentration of cCPA, although this ratio may be an underestimation as the cCPA concentration in the hippocampus is expected to follow a gradient, with the highest concentrations at its borders adjacent to the ventricle and lower concentrations at the site of recording in the dentate gyrus. Anyhow, our *in vivo* experiments required relatively high doses of cCPA and repeated light flashes to achieve clear inhibitory effects of A_1R activation.

Besides validating the photopharmacological modulation of hippocampal excitability through photo-release of CPA, the first proof of concept experiments have also been performed to showcase the anticonvulsive potential of light-mediated A_1R activation. In recent *ex vivo* experiments with the high-potassium slice model of epilepsy, we were able to suppress epileptiform bursts by controlling hippocampal excitability using photo-released CPA [37]. Now, we also expanded these findings to an *in vivo* epilepsy model, by testing photopharmacological suppression of spontaneous seizures in the IHKA mouse model. Our results with cCPA demonstrate the therapeutic potential of local A_1R modulation, as photo-releasing CPA in the sclerotic hippocampus strongly suppresses seizures. In several of the animals, the occurrence of seizures was even completely suppressed during the entire 2-h illumination period. As revealed in our exploratory pharmacokinetic analysis, cCPA possesses a relatively long half-life in the brain of >3 h, explaining the ability to obtain such a sustained suppression of seizures after a single injection of cCPA. Seizure suppression was only achieved when cCPA was combined with local illumination and control recordings with the photocage DEACM also confirmed that the effects were not due to any potential antiseizure activity of the coumarin derivative [54–56]. Gouder et al. were the first to show that administration of an A_1R agonist can effectively suppress seizures in this mouse model of DRE [18]. In their study, 2-chloro-N^6-cyclopentyladenosine was administered intraperitoneally together with a non-brain permeable antagonist to demonstrate that the suppression is due to central A_1R activation. This approach was, however, affecting receptors throughout the entire CNS. The authors already suggested that local delivery of adenosine into the brain could be effective for the treatment of DRE, as earlier studies had shown that focal injections of adenosine or synthetic analogues had anticonvulsive effects in different epilepsy models [4,6,8,57,58]. Unfortunately, the spatial arrangement of our implantation configuration prevented local injections of CPA as a positive control, which is a limitation of this study. Nonetheless, our current study confirms that more locally targeted A_1R receptor modulation is indeed effective at suppressing seizures in this model for DRE.

As one of the main advantages of this photopharmacological approach would be to avoid side effects by targeting A_1R activation primarily in the epileptic focus, we investigated whether this would have less sedative effects compared to CPA administration. With the current dose of cCPA and illumination protocol, the photopharmacological treatment led to an overall better performance on the accelerating rotarod compared to CPA administration, which caused a

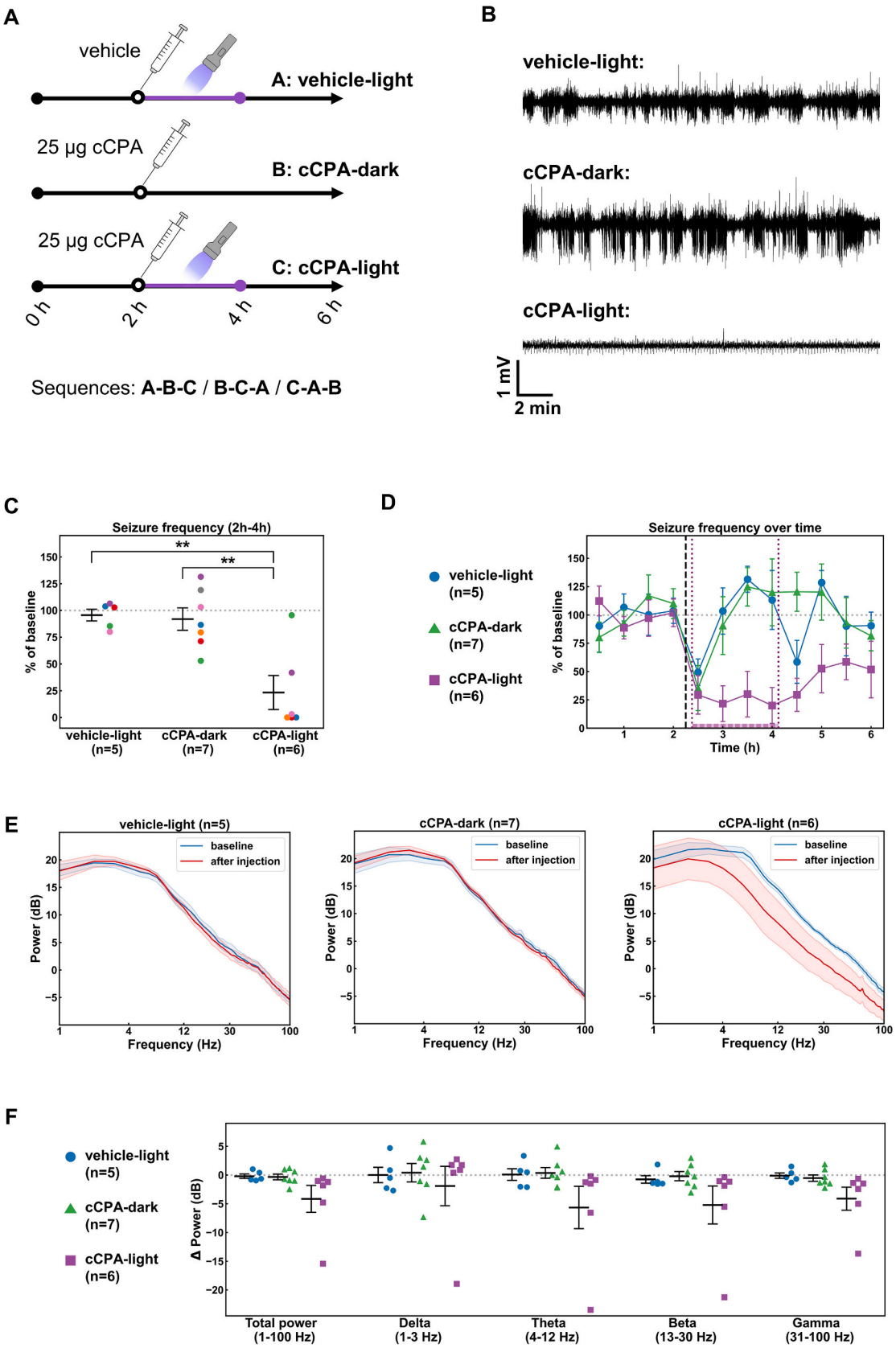

(caption on next page)

Fig. 6. Effects of photo-releasing CPA on epileptic seizures and interictal electroencephalography (EEG). (**A**) Design of the cross-over experiment with cCPA in the intrahippocampal kainic acid (IHKA) model. Animals were randomly assigned to 1 out of 3 sequences to receive 3 treatments: ICV injection of vehicle with 405 nm illumination (vehicle-light), ICV injection of 25 μg cCPA without illumination (cCPA-dark) and 25 μg cCPA with illumination (cCPA-light). Injections were performed after 2 h of baseline EEG recording, followed by 2 h of pulsed 405 nm illumination in the vehicle-light and cCPA-light treatments. Two days of wash-out were implemented between treatments. (**B**) Examples of 20-min EEG segments after administration of the 3 treatments in an animal with complete seizure suppression in the cCPA-light treatment. (**C**) Effects on average seizure frequency during the 2-h period after injection for the vehicle-light ($n = 5$), cCPA-dark ($n = 7$) and cCPA-light ($n = 6$) treatments. Results of individual animals for each treatment are represented by marks colour-coded for each animal. ** indicates $p < 0.01$. (**D**) Effects on seizure frequency over time of the 3 treatments, plotted per 30 min. Dashed line indicates time of injection, dotted lines indicate start and end of illumination in the vehicle-light and cCPA-light groups. (**E**) Power spectra of the interictal EEG before (blue) and after (red) administration of the 3 treatments. (**F**) Change in interictal EEG power compared to baseline in the different frequency bands (total power:1–100 Hz, delta power:1–3 Hz, theta power: 4–12 Hz, beta power: 13–30 Hz, gamma power: 31–100 Hz). Results of individual animals are represented by marks. (For interpretation of the references to colour in this figure legend, the reader is referred to the web version of this article.)

clear impairment in all animals. However, local photo-release of CPA was not completely free of side effects as in some animals signs of sedation and decreased locomotor activity did occur. In 2 animals, sedation and suppression of EEG after cCPA-light treatment were on a similar level to that after administration of CPA. The most likely explanation would be that in these mice too much cCPA was uncaged and/or leaking into other brain regions. Potentially, light reaching the ventricles surrounding the hippocampus could cause photo-release of higher amounts of CPA inside the cerebrospinal fluid (CSF), leading to similar effects as ICV administration of CPA. Importantly though, such sedative effects were not witnessed in the prior experiments with the cCPA-light treatment in any of the IHKA mice, indicating that seizure suppression did not rely on such off-target or excessive release of CPA. However, further fine-tuning of our current photopharmacological protocol, *e.g.* by adjusting illumination parameters based on light propagation models [59,60], will be required in future work to minimize the occurrence of such side effects.

Throughout the various experiments, we also examined effects on hippocampal EEG. Overall, administration of cCPA caused no effect in the absence of illumination, while A_1R activation either with direct administration or with photo-release of CPA caused a decrease in EEG power. Due to the difference in experimental settings, the effects did vary between experiments. In healthy anesthetized mice, ICV injection of CPA caused a larger decrease in EEG power compared to photo-release of CPA. While the cCPA-light condition caused a small decrease ranging between 2.3 and 3.3 dB in power across all frequency bands, CPA decreased the power of beta and gamma frequencies by 2.5 to 8.2 dB and showed the most pronounced effects in the delta and theta band frequency ranges, which were reduced by 10.5 to 13.1 dB. The profound power decrease in the delta/theta frequency bands in case of ICV injection of CPA could point towards a more widespread effect compared to local photo-release of CPA, as low frequency EEG activity is thought to be generated by large-scale neuronal network activity while fast oscillations represent the activity of local neuronal assemblies [61,62]. In epileptic animals, photo-releasing CPA also caused a small decrease in interictal EEG power. In these EEG recordings, power in the delta band was reduced by 1.9 dB while the higher frequencies were affected more significantly, displaying decreases ranging between 4.1 and 5.6 dB, again suggesting a primarily local effect. In healthy animals which showed severe deterioration of performance in the rotarod test upon ICV CPA administration, >10 dB decreases in EEG power across the different bands upon CPA administration were found. This also occurred in the two mice that were sedated in the cCPA-light conditions, indicative of the sedative effects of widespread A_1R activation.

The exploratory pharmacokinetic investigation of this new photocaged compound also provided some first insights regarding the stability of cCPA *in vivo*. No CPA was measured in hippocampus and blood samples, which would suggest that cCPA remains stable at these sites. Indeed, no effects were observed on hippocampal excitability or behavior in the cCPA-dark control groups across the various experiments. However, low concentrations of CPA were present in the brain samples, indicating a small fraction of cCPA (approximately 0.5 %) was converted to CPA. The currently measured concentrations of CPA in brain samples, around 11 nM at its maximum, would be expected to cause some effects through A_1R activation. Yet, our current analysis does not allow us to distinguish where in the brain exactly this amount of CPA would be situated.

5. Future perspectives and conclusion

This study provides a first proof of concept for *in vivo* light-controlled activation of A_1R signaling with our novel caged A_1R agonist. There are several limitations to this study and multiple important questions remain that will require further study to develop this photopharmacological approach beyond a proof of concept. Some important current limitations are the lack of knowledge about the biodistribution of cCPA to other organs and the pharmacokinetics of CPA after photo-uncaging. Based on *ex vivo* data the amount of active CPA that was released after photo-uncaging can be roughly estimated to be in the nanomolar range. Besides the question of how much CPA is released, further detailed investigations will also need to address the temporal and spatial resolution of photo-uncaging, investigating the extent of CPA diffusion after photo-release and the duration of activity of the uncaged compound. Adenosine analogues are more resistant to metabolization and half-life values of CPA determined in the blood of rats have been reported to be 24 min *in vitro* and 7 min *in vivo* [63,64]. It could thus be possible that after local photo-uncaging, there is enough time for the released CPA to diffuse outside of the targeted region and spread *via* systemic circulation. As our current results lead us to estimate that only a very low concentration of CPA is released, concentrations possibly reaching the bloodstream would be miniscule. Additionally, the low amounts of cCPA measured in the blood lead us to believe that the spread of cCPA to other major organs will be limited with the current approach. However, it will be important to validate cCPA/CPA concentrations and the absence of side effects on multiple organ systems, such as bradycardia and hypothermia.

Here, our photopharmacological approach was executed in acute experiments. Since epilepsy is a chronic disorder, the aim is to further develop this approach into a chronic treatment option. Previous studies have investigated different strategies for chronic local delivery of adenosine, but this involved a continuous slow infusion or release of adenosine [65]. With our photopharmacological approach, we aim to investigate chronic delivery of cCPA to achieve a stable concentration of the inactive compound in the brain. Ideally, this would be achieved in a less invasive manner *via* systemic administration. Further studies could include microdialysis combined with the investigation of effects on EEG and behavior. Insight in the changes of local levels of cCPA provided by microdialysis would allow fine-tuning of cCPA dosing and illumination protocols for photo-release of CPA. It could then be determined which levels of CPA photo-release are optimal and result in suppression of seizures while minimizing cognitive side-effects that could occur due to the suppression of local neuronal activity. Apart from the possibility to locally activate the drug to avoid systemic side-effects, photopharmacology also offers the advantage of strong temporal control. The light-mediated uncaging would provide a fast release of CPA in the targeted brain region. Additionally, it would allow to modulate A_1Rs

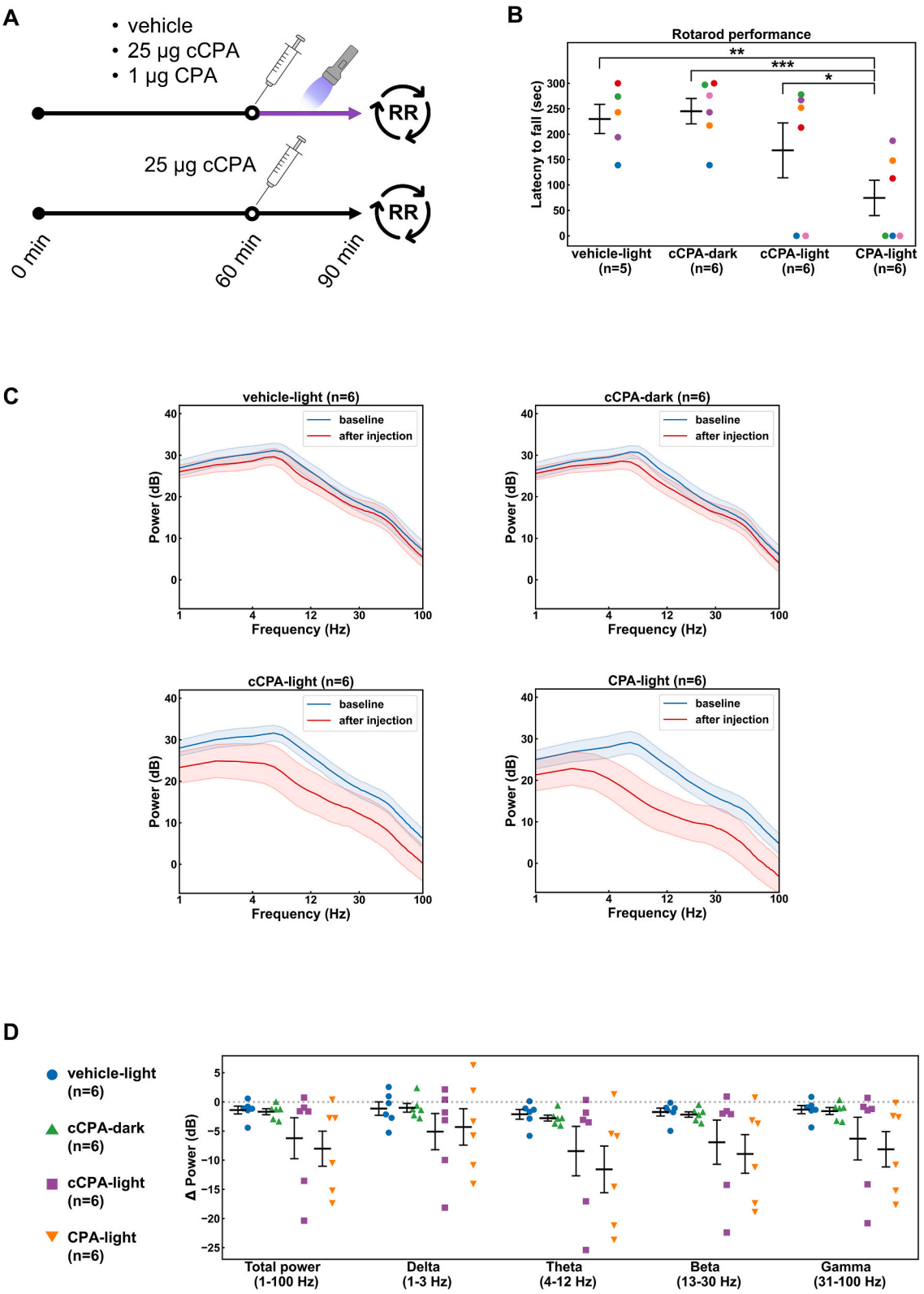

Fig. 7. Effects of CPA and cCPA administration on rotarod performance and electroencephalography (EEG) power. (**A**) Protocol of the EEG recordings and rotarod (RR) trials: after 1 h of baseline EEG recording, animals received an ICV injection of either vehicle with 405 nm illumination (vehicle-light), 25 µg cCPA without illumination (cCPA-dark), 25 µg cCPA with illumination (cCPA-light) or 1 µg CPA with illumination (CPA-light). EEG was recorded for 30 min after injection, after which animals were placed on the rotarod. (**B**) Effects on rotarod performance 30 min after injection for the vehicle-light ($n = 5$), cCPA-dark ($n = 6$), cCPA-light (n = 6) and CPA-light (n = 6) treatments. Results of individual animals for each treatment are represented by marks colour-coded for each animal. * indicates $p < 0.05$, ** indicates $p < 0.01$, *** indicates $p < 0.001$. (**C**) EEG power spectra before (blue) and after (red) ICV injection for the 4 treatments. (**D**) Change in EEG power compared to baseline in the different frequency bands (total power:1–100 Hz, delta power:1–3 Hz, theta power: 4–12 Hz, beta power: 13–30 Hz, gamma power: 31–100 Hz). Results of individual animals are represented by marks. (For interpretation of the references to colour in this figure legend, the reader is referred to the web version of this article.)

only when required, avoiding sustained receptor activation which could induce receptor desensitization and reduce efficacy. Photopharmacological modulation could be well-suited for integration with a closed-loop system, where interventions are placed under automatic control of a detection system monitoring physiological parameters of interest [66–68]. This concept was investigated in our lab in an *ex vivo* setting [37,69]. Caged CPA was used together with feedback-controlled light delivery to keep neurotransmission, monitored *via* fEPSP amplitude, to a predefined level. Similarly, cCPA could be used *in vivo* to stabilize the level of excitability and prevent seizures, either through monitoring of EP amplitudes or through EEG registration combined with seizure prediction algorithms. This would allow for a more titrated release of CPA, possibly further decreasing the chance of sedative and cognitive effects.

Future clinical translation of this envisioned therapy will rely on many more developments. The use of chronic systemic administration will demand the study of the effects of long-term exposure, requiring more in-depth investigations into the biodistribution of the caged compound before and after photo-uncaging. Further development of next-generation caged agonists will be essential as well. These will need to be optimized for efficient passage across the blood-brain barrier and stability, with a longer wavelength-sensitivity more suitable for *in vivo* applications. Upscaling of the experiments to larger animal models and eventually patients may require more intricate illumination set-ups, for which multiple or more advanced waveguides (*e.g.* tapered fibers) could be used to illuminate larger brain volumes [70]. Furthermore, biocompatibility and invasiveness of light delivery into the brain will also remain an important challenge, but has already seen major improvements [71]. Fortunately, as the multidisciplinary field of photopharmacology is becoming increasingly popular, extensive progress is being made enabling more and more *in vivo* applications and bridging the gaps towards clinical translation.

In conclusion, with this work we presented the first application of a photocaged A_1R agonist *in vivo*. We demonstrated that this caged agonist is inactive upon ICV administration and that it is possible to locally release the agonist with focused illumination in the hippocampus of mice, achieving a reduction of hippocampal neurotransmission and significant suppression of spontaneous seizures in the IHKA mouse model for DRE. This proof of concept study showcases the therapeutic potential of photopharmacology, as it allows us to take advantage of the potent anticonvulsive effects of the adenosinergic system in a way that can be further developed to achieve minimal side effects through the high spatiotemporal control afforded by light.

Funding

This research was funded by Research Foundation Flanders-FWO (grant numbers 1S32321N, G042219N and G088519N) and by the Ghent University Special Research Fund-BOF (grant number 01G02722).

CRediT authorship contribution statement

Jeroen Spanoghe: Writing – original draft, Visualization, Methodology, Investigation, Formal analysis, Conceptualization. **Evelien Wynendaele:** Formal analysis, Investigation, Methodology, Writing – review & editing. **Marijke Vergaelen:** Writing – review & editing, Methodology, Conceptualization. **Maren De Colvenaer:** Investigation, Formal analysis. **Tina Mariman:** Investigation, Formal analysis. **Kristl Vonck:** Writing – review & editing, Supervision, Funding acquisition, Conceptualization. **Wytse Wadman:** Writing – review & editing, Software, Conceptualization. **Erine Craey:** Writing – review & editing, Methodology, Conceptualization. **Lars E. Larsen:** Software, Formal analysis, Conceptualization. **Mathieu Sprengers:** Writing – review & editing, Conceptualization. **Jeroen Missinne:** Writing – review & editing, Resources. **Serge Van Calenbergh:** Writing – review & editing, Resources, Methodology. **Bart De Spiegeleer:** Methodology, Resources. **Dimitri De Bundel:** Writing – review & editing, Funding acquisition, Conceptualization. **Ilse Smolders:** Writing – review & editing, Funding acquisition, Conceptualization. **Paul Boon:** Supervision, Project administration, Funding acquisition, Conceptualization. **Robrecht Raedt:** Writing – review & editing, Supervision, Project administration, Funding acquisition, Conceptualization.

Declaration of competing interest

None.

Data availability

Data will be made available on request.

Acknowledgements

The authors thank the Core ARTH Animal Facilities (BOF/COR/2022/007) at Ghent University for the provision and care of animals. The following people are kindly thanked for their assistance with part of the experiments: Robin Lefevere, Lien De Schaepmeester, Anastasiia Babych, Sielke Caestecker, Dina K.C. and Laure De Smet. Figures were partially created with Biorender.com.

Appendix A. Supplementary data

Supplementary data to this article can be found online at https://doi.org/10.1016/j.jconrel.2025.113626.

References

[1] C. Behr, M.A. Goltzene, G. Kosmalski, E. Hirsch, P. Ryvlin, Epidemiology of epilepsy, Rev. Neurol. (Paris) 172 (1) (2016) 27–36, https://doi.org/10.1016/j.neurol.2015.11.003.
[2] K.M. Fiest, K.M. Sauro, S. Wiebe, et al., Prevalence and incidence of epilepsy, Neurology 88 (3) (2017) 296–303, https://doi.org/10.1212/WNL.0000000000003509.
[3] B. Sultana, M.-A. Panzini, A. Veilleux Carpentier, et al., Incidence and prevalence of drug-resistant epilepsy, Neurology 96 (17) (2021) 805–817, https://doi.org/10.1212/WNL.0000000000011839.
[4] P.H. Franklin, G. Zhang, E.D. Tripp, T.F. Murray, Adenosine A1 receptor activation mediates suppression of (−) bicuculline methiodide-induced seizures in rat prepiriform cortex, J. Pharmacol. Exp. Ther. 251 (3) (1989) 1229–1236. http://www.ncbi.nlm.nih.gov/pubmed/2600813. (Accessed 29 January 2020).
[5] D.K.J.E. Von Lubitz, I.A. Paul, M. Carter, K.A. Jacobson, Effects of N6-cyclopentyl adenosine and 8-cyclopentyl-1,3-dipropylxanthine on induced seizures in mice, Eur. J. Pharmacol. 249 (3) (1993) 265–270, https://doi.org/10.1016/0014-2999(93)90521-I.
[6] A.-S. Abdul-Ghani, P.J.E. Attwell, H.F. Bradford, The protective effect of 2-chloroadenosine against the development of amygdala kindling and on amygdala-kindled seizures, Eur. J. Pharmacol. 326 (1) (1997) 7–14, https://doi.org/10.1016/S0014-2999(97)00139-8.
[7] D.E. Fedele, T. Li, J.Q. Lan, B.B. Fredholm, D. Boison, Adenosine A1 receptors are crucial in keeping an epileptic focus localized, Exp. Neurol. 200 (1) (2006) 184–190, https://doi.org/10.1016/j.expneurol.2006.02.133.
[8] A. Van Dycke, R. Raedt, I. Dauwe, et al., Continuous local intrahippocampal delivery of adenosine reduces seizure frequency in rats with spontaneous seizures, Epilepsia 51 (9) (2010) 1721–1728, https://doi.org/10.1111/j.1528-1167.2010.02700.x.
[9] G.M. Khan, I. Smolders, G. Ebinger, Y. Michotte, Anticonvulsant effect and neurotransmitter modulation of focal and systemic 2-chloroadenosine against the development of pilocarpine-induced seizures, Neuropharmacology 39 (12) (2000) 2418–2432, https://doi.org/10.1016/S0028-3908(00)00072-1.
[10] G.M. Khan, U. Smolders, G. Ebinger, Y. Michotte, 2-Chloro-N6-cyclopentyladenosine-elicited attenuation of evoked glutamate release is not sufficient to give complete protection against pilocarpine-induced seizures in rats, Neuropharmacology 40 (5) (2001) 657–667, https://doi.org/10.1016/S0028-3908(00)00203-3.
[11] Z.J. Klaft, L.M. Duerrwald, Z. Gerevich, C.G. Dulla, The adenosine A1 receptor agonist WAG 994 suppresses acute kainic acid-induced status epilepticus in vivo, Neuropharmacology 176 (2020) 108213, https://doi.org/10.1016/j.neuropharm.2020.108213.
[12] H.R. Winn, J.E. Welsh, R. Rubio, R.M. Berne, Changes in brain adenosine during bicuculline-induced seizures in rats. Effects of hypoxia and altered systemic blood

pressure, Circ. Res. 47 (4) (1980) 568–577, https://doi.org/10.1161/01.RES.47.4.568.
[13] J. Schrader, M. Wahl, W. Kuschinsky, G.W. Kreutzberg, Increase of adenosine content in cerebral cortex of the cat during bicuculline-induced seizure, Pflugers Arch. - Eur. J. Physiol. 387 (3) (1980) 245–251, https://doi.org/10.1007/BF00580977.
[14] M.J. During, D.D. Spencer, Adenosine: a potential mediator of seizure arrest and postictal refractoriness, Ann. Neurol. 32 (5) (1992) 618–624, https://doi.org/10.1002/ana.410320504.
[15] J. Spanoghe, L.E. Larsen, E. Craey, et al., The signaling pathways involved in the anticonvulsive effects of the adenosine a1 receptor, Int. J. Mol. Sci. 22 (1) (2021) 1–26, https://doi.org/10.3390/ijms22010320.
[16] P. Svenningsson, H. Hall, G. Sedvall, B.B. Fredholm, Distribution of adenosine receptors in the postmortem human brain: an extended autoradiographic study, Synapse 27 (4) (1997) 322–335, https://doi.org/10.1002/(SICI)1098-2396(199712)27:4<322::AID-SYN6>3.0.CO;2-E.
[17] J. Sheng, S. Liu, H. Qin, B. Li, X. Zhang, Drug-resistant epilepsy and surgery, Curr. Neuropharmacol. 16 (1) (2018) 17–28, https://doi.org/10.2174/1570159X15666170504123316.
[18] N. Gouder, J.-M. Fritschy, D. Boison, Seizure suppression by adenosine A1 receptor activation in a mouse model of Pharmacoresistant epilepsy, Epilepsia 44 (7) (2003) 877–885, https://doi.org/10.1046/j.1528-1157.2003.03603.x.
[19] Z.J. Klaft, J.O. Hollnagel, S. Salar, et al., Adenosine A1 receptor-mediated suppression of carbamazepine-resistant seizure-like events in human neocortical slices, Epilepsia 57 (5) (2016) 746–756, https://doi.org/10.1111/epi.13360.
[20] D. Boison, L. Scheurer, J.L. Tseng, P. Aebischer, H. Mohler, Seizure suppression in kindled rats by intraventricular grafting of an adenosine releasing synthetic polymer, Exp. Neurol. 160 (1) (1999) 164–174, https://doi.org/10.1006/exnr.1999.7209.
[21] C. Szybala, E.M. Pritchard, T.A. Lusardi, et al., Antiepileptic effects of silk-polymer based adenosine release in kindled rats, Exp. Neurol. 219 (1) (2009) 126–135, https://doi.org/10.1016/j.expneurol.2009.05.018.
[22] A. Huber, V. Padrun, N. Déglon, P. Aebischer, H. Möhler, D. Boison, Grafts of adenosine-releasing cells suppress seizures in kindling epilepsy, Proc. Natl. Acad. Sci. USA 98 (13) (2001) 7611–7616, https://doi.org/10.1073/pnas.131102898.
[23] M. Güttinger, D. Fedele, P. Koch, et al., Suppression of kindled seizures by paracrine adenosine release from stem cell-derived brain implants, Epilepsia 46 (8) (2005) 1162–1169, https://doi.org/10.1111/j.1528-1167.2005.61804.x.
[24] T. Li, J.A. Steinbeck, T. Lusardi, et al., Suppression of kindling epileptogenesis by adenosine releasing stem cell-derived brain implants, Brain 130 (5) (2007) 1276–1288, https://doi.org/10.1093/brain/awm057.
[25] M.W.H. Hoorens, W. Szymanski, Reversible, spatial and temporal control over protein activity using light, Trends Biochem. Sci. 43 (8) (2018) 567–575, https://doi.org/10.1016/j.tibs.2018.05.004.
[26] M. Ricart-Ortega, J. Font, A. Llebaria, GPCR photopharmacology, Mol. Cell. Endocrinol. 488 (2019) 36–51, https://doi.org/10.1016/j.mce.2019.03.003.
[27] P.D. Bregestovski, G.V. Maleeva, Photopharmacology: a brief review using the control of potassium channels as an example, Neurosci. Behav. Physiol. 49 (2) (2019) 184–191, https://doi.org/10.1007/s11055-019-00713-3.
[28] J. Font, M. López-Cano, S. Notartomaso, et al., Optical control of pain in vivo with a photoactive mGlu5 receptor negative allosteric modulator, Elife (2017) 6, https://doi.org/10.7554/eLife.23545.
[29] M. López-Cano, J. Font, E. Aso, et al., Remote local photoactivation of morphine produces analgesia without opioid-related adverse effects, Br. J. Pharmacol. 180 (7) (2023) 958–974, https://doi.org/10.1111/bph.15645.
[30] S.P. McClain, X. Ma, D.A. Johnson, et al., In vivo photopharmacology with light-activated opioid drugs, Neuron 111 (24) (2023) 3926–3940.e10, https://doi.org/10.1016/j.neuron.2023.09.017.
[31] J. Taura, E.G. Nolen, G. Cabré, et al., Remote control of movement disorders using a photoactive adenosine a 2A receptor antagonist, J. Control. Release 283 (2018) 135–142, https://doi.org/10.1016/j.jconrel.2018.05.033.
[32] M. López-Cano, I. Filgaira, E.G. Nolen, et al., Optical control of adenosine A3 receptor function in psoriasis, Pharmacol. Res. 170 (2021) 105731, https://doi.org/10.1016/J.PHRS.2021.105731.
[33] X. Yang, D.L. Rode, D.S. Peterka, R. Yuste, S.M. Rothman, Optical control of focal epilepsy in vivo with caged γ-aminobutyric acid, Ann. Neurol. 71 (1) (2012) 68, https://doi.org/10.1002/ANA.22596.
[34] D. Wang, Z. Yu, J. Yan, et al., Photolysis of caged-GABA rapidly terminates seizures in vivo: concentration and light intensity dependence, Front. Neurol. (2017) 8 (MAY), https://doi.org/10.3389/fneur.2017.00215.
[35] P. Klán, T. Šolomek, C.G. Bochet, et al., Photoremovable protecting groups in chemistry and biology: reaction mechanisms and efficacy, Chem. Rev. 113 (1) (2013) 119–191, https://doi.org/10.1021/cr300177k.
[36] E. Craey, F. Hulpia, J. Spanoghe, et al., Ex vivo feedback control of neurotransmission using a Photocaged adenosine A1 receptor agonist, Int. J. Mol. Sci. 23 (16) (2022), https://doi.org/10.3390/ijms23168887.
[37] E. Craey, Calenbergh S. Van, J. Spanoghe, et al., Feedback control of neuronal excitability and epileptiform bursting using a Photocaged adenosine A1 agonist, bioRxiv (June 2024), https://doi.org/10.1101/2024.06.17.597004, 2024.06.17.597004.
[38] K. Payne, C.J. Wilson, S. Young, E. Fifkova, P.M. Groves, Evoked potentials and long-term potentiation in the mouse dentate gyrus after stimulation of the entorhinal cortex, Exp. Neurol. 75 (1) (1982) 134–148, https://doi.org/10.1016/0014-4886(82)90013-9.
[39] V. Bouilleret, V. Ridoux, A. Depaulis, C. Marescaux, A. Nehlig, Le Gal La Salle, G., Recurrent seizures and hippocampal sclerosis following intrahippocampal kainate injection in adult mice: electroencephalography, histopathology and synaptic reorganization similar to mesial temporal lobe epilepsy, Neuroscience 89 (3) (1999) 717–729, https://doi.org/10.1016/S0306-4522(98)00401-1.
[40] V. Riban, V. Bouilleret, B.T. Pham-Lê, J.M. Fritschy, C. Marescaux, A. Depaulis, Evolution of hippocampal epileptic activity during the development of hippocampal sclerosis in a mouse model of temporal lobe epilepsy, Neuroscience 112 (1) (2002) 101–111, https://doi.org/10.1016/S0306-4522(02)00064-7.
[41] J.N. Crawley, J. Patel, P.J. Marangos, Behavioral characterization of two long-lasting adenosine analogs: sedative properties and interaction with diazepam, Life Sci. 29 (25) (1981) 2623–2630, https://doi.org/10.1016/0024-3205(81)90636-6.
[42] T.V. Dunwiddie, T. Worth, Sedative and anticonvulsant effects of adenosine analogs in mouse and rat, J. Pharmacol. Exp. Ther. 220 (1) (1982) 70–76. http://www.ncbi.nlm.nih.gov/pubmed/7053424. Accessed April 28, 2020.
[43] R. Anderson, M.J. Sheehan, P. Strong, Characterization of the adenosine receptors mediating hypothermia in the conscious mouse, Br. J. Pharmacol. 113 (4) (1994) 1386–1390, https://doi.org/10.1111/j.1476-5381.1994.tb17151.x.
[44] B.J. Jones, D.J. Roberts, The quantitative measurement of motor inco-ordination in naive mice using an accelerating rotarod, J. Pharm. Pharmacol. 20 (4) (1968) 302–304, https://doi.org/10.1111/j.2042-7158.1968.tb09743.x.
[45] G. Bureau, M. Carrier, M. Lebel, M. Cyr, Intrastriatal inhibition of extracellular signal-regulated kinases impaired the consolidation phase of motor skill learning, Neurobiol. Learn. Mem. 94 (1) (2010) 107–115, https://doi.org/10.1016/j.nlm.2010.04.008.
[46] S. Boutaleb, J.P. Pouget, C. Hindorf, et al., Impact of mouse model on preclinical dosimetry in targeted radionuclide therapy, Proc. IEEE 97 (12) (2009) 2076–2085, https://doi.org/10.1109/JPROC.2009.2026921.
[47] H.J. Cho, S.H. Eo, Outlier detection for mass spectrometric data, Methods Mol. Biol. 1362 (2016) 91–102, https://doi.org/10.1007/978-1-4939-3106-4_5/FIGURES/7.
[48] S.L. Mironov, K. Langohr, D.W. Richter, A1 adenosine receptors modulate respiratory activity of the neonatal mouse via the cAMP-mediated signaling pathway, J. Neurophysiol. 81 (1) (1999) 247–255, https://doi.org/10.1152/JN.1999.81.1.247/ASSET/IMAGES/LARGE/JNP.JA11F10.JPEG.
[49] M. Sharma, S.H. Friedman, The issue of tissue: approaches and challenges to the light control of drug activity, ChemPhotoChem (2021), https://doi.org/10.1002/cptc.202100001.
[50] F. Fahoum, S. Eyal, Intracerebroventricular administration for delivery of antiseizure therapeutics: challenges and opportunities, Epilepsia 64 (7) (2023) 1750–1765, https://doi.org/10.1111/epi.17625.
[51] N. Rebola, J.E. Coelho, A.R. Costenla, et al., Decrease of adenosine A1 receptor density and of adenosine neuromodulation the hippocampus of kindled rats, Eur. J. Neurosci. 18 (4) (2003) 820–828, https://doi.org/10.1046/j.1460-9568.2003.02815.x.
[52] A.M. Sebastião, R.A. Cunha, A. De Mendonça, J.A. Ribeiro, Modification of adenosine modulation of synaptic transmission in the hippocampus of aged rats, Br. J. Pharmacol. 131 (8) (2000) 1629–1634, https://doi.org/10.1038/sj.bjp.0703736.
[53] A. De Mendonça, J.A. Ribeiro, Influence of metabotropic glutamate receptor agonists on the inhibitory effects of adenosine A1 receptor activation in the rat hippocampus, Br. J. Pharmacol. 121 (8) (1997) 1541–1548, https://doi.org/10.1038/sj.bjp.0701291.
[54] K. Skalicka-Woźniak, I.E. Orhan, G.A. Cordell, S.M. Nabavi, B. Budzyńska, Implication of coumarins towards central nervous system disorders, Pharmacol. Res. 103 (2016) 188–203, https://doi.org/10.1016/J.PHRS.2015.11.023.
[55] J. Bryda, M. Zagaja, A. Szewczyk, M. Andres-Mach, Coumarins as potential supportive medication for the treatment of epilepsy, Acta Neurobiol. Exp. (Wars) 79 (2) (2019) 126–132, https://doi.org/10.21307/ane-2019-011.
[56] E. Kozioł, K. Jóźwiak, B. Budzyńska, P.A.M. de Witte, D. Copmans, K. Skalicka-woźniak, Comparative antiseizure analysis of diverse natural coumarin derivatives in zebrafish, Int. J. Mol. Sci. 22 (21) (2021) 11420, https://doi.org/10.3390/ijms222111420.
[57] J.B. Rosen, R.F. Berman, Differential effects of adenosine analogs on amygdala, Hippocampus, and caudate nucleus kindled seizures, Epilepsia 28 (6) (1987) 658–666, https://doi.org/10.1111/j.1528-1157.1987.tb03697.x.
[58] G. Zhang, P.H. Franklin, T.F. Murray, Manipulation of endogenous adenosine in the rat prepiriform cortex modulates seizure susceptibility, J. Pharmacol. Exp. Ther. 264 (3) (1993).
[59] Y. Shin, M. Yoo, H.-S. Kim, et al., Characterization of fiber-optic light delivery and light-induced temperature changes in a rodent brain for precise optogenetic neuromodulation, Biomed. Opt. Express 7 (11) (2016) 4450, https://doi.org/10.1364/boe.7.004450.
[60] G. Yona, N. Meitav, I. Kahn, S. Shoham, Realistic numerical and analytical modeling of light scattering in brain tissue for optogenetic applications, eNeuro 3 (1) (2016) 420–424, https://doi.org/10.1523/ENEURO.0059-15.2015.
[61] J.E. Lisman, O. Jensen, The Theta-gamma neural code, Neuron 77 (6) (2013) 1002–1016, https://doi.org/10.1016/j.neuron.2013.03.007.
[62] A. von Stein, J. Sarnthein, Different frequencies for different scales of cortical integration: from local gamma to long range alpha/theta synchronization, Int. J. Psychophysiol. 38 (3) (2000) 301–313, https://doi.org/10.1016/S0167-8760(00)00172-0.
[63] R.A.A. Mathôt, S. Appel, E.A. van Schaick, W. Soudijn, A.P. Ijzerman, M. Danhof, High-performance liquid chromatography of the adenosine A1 agonist N6-cyclopentyladenosine and the A1 antagonist 8-cyclopentyltheophylline and its application in a pharmacokinetic study in rats, J. Chromatogr. B Biomed. Sci. Appl. 620 (1) (1993) 113–120, https://doi.org/10.1016/0378-4347(93)80058-C.

[64] E.A. Van Schaick, R.A.A. Mathôt, J.M. Gubbens-Stibbe, et al., 8-Alkylamino-substituted analogs of N6-cyclopentyladenosine are partial agonists for the cardiovascular adenosine A1 receptors in vivo, J. Pharmacol. Exp. Ther. 283 (2) (1997) 800–808.
[65] A. Van Dycke, R. Raedt, K. Vonck, P. Boon, Local delivery strategies in epilepsy; A focus on adenosine, Seizure 20 (5) (2011) 376–382, https://doi.org/10.1016/j.seizure.2011.03.003.
[66] S. Zanos, Closed-Loop Neuromodulation in Physiological and Translational Research vol. 9(11), Cold Spring Harb Perspect Med, 2019, https://doi.org/10.1101/cshperspect.a034314.
[67] W. Kang, C. Ju, J. Joo, J. Lee, Y.M. Shon, S.M. Park, Closed-loop direct control of seizure focus in a rodent model of temporal lobe epilepsy via localized electric fields applied sequentially, Nat. Commun. 13 (1) (2022) 1–18, https://doi.org/10.1038/s41467-022-35540-7.
[68] M. Zare, M. Rezaei, M. Nazari, et al., Effect of the closed-loop hippocampal low-frequency stimulation on seizure severity, learning, and memory in pilocarpine epilepsy rat model, CNS Neurosci. Ther. 30 (3) (2024) e14656, https://doi.org/10.1111/CNS.14656.
[69] E. Craey, F. Hulpia, J. Spanoghe, et al., Ex vivo feedback control of neurotransmission using a Photocaged adenosine A1 receptor agonist, Int. J. Mol. Sci. 23 (16) (2022) 8887, https://doi.org/10.3390/ijms23168887.
[70] S. Pearson, J. Feng, A. del Campo, Lighting the path: light delivery strategies to activate Photoresponsive biomaterials in vivo, Adv. Funct. Mater. (2021) 2105989, https://doi.org/10.1002/ADFM.202105989.
[71] R. Nazempour, Q. Zhang, R. Fu, X. Sheng, Biocompatible and implantable optical fibers and waveguides for biomedicine, Materials (Basel). 11 (8) (2018) 1283, https://doi.org/10.3390/ma11081283.